AMERICAN UNIVERSITY OF BEIRUT

SURFACE MODIFICATION OF ELECTROSPUN POLY(VINYL CHLORIDE) MEMBRANE FOR OIL-WATER SEPARATION

by
RAZAN ALI BADRAN

A thesis
Submitted in partial fulfillment of the requirements
for the degree of Master of Engineering
to the Baha and Walid Bassatne Department of Chemical Engineering and Advanced Energy
of the Maroun Semaan Faculty of Engineering and Architecture
at the American University of Beirut

Beirut, Lebanon
September 2019

AMERICAN UNIVERSITY OF BEIRUT

Surface Modification of Polyvinyl Chloride (PVC) Electrospun Membrane for Oil-Water Separation

by

RAZAN ALI BADRAN

Approved by:

Ali Tehrani

Dr. Ali Tehrani, Professor — Advisor
Department of Chemical Engineering and Advanced Energy

Dr. Kamel Aboughali, Professor — Co-Advisor
Department of Mechanical Engineering

Dr. Mohammad N. Ahmad, Professor, Chairman — Member of Committee
Department of Chemical Engineering and Advanced Energy

Dr. Nesreen Ghaddar, Professor — Member of Committee
Department of Mechanical Engineerig

Date of thesis defense: September 5, 2019

AMERICAN UNIVERSITY OF BEIRUT

THESIS, DISSERTATION, PROJECT RELEASE FORM

Student Name: Badran Razan Ali
Last First Middle

☑ Master's Thesis ○ Master's Project ○ Doctoral Dissertation

☐ I authorize the American University of Beirut to: (a) reproduce hard or electronic copies of my thesis, dissertation, or project; (b) include such copies in the archives and digital repositories of the University; and (c) make freely available such copies to third parties for research or educational purposes.

☑ I authorize the American University of Beirut, to: (a) reproduce hard or electronic copies of it; (b) include such copies in the archives and digital repositories of the University; and (c) make freely available such copies to third parties for research or educational purposes after:

One ✓ year from the date of submission of my thesis.
Two ---- years from the date of submission of my thesis.
Three ---- years from the date of submission of my thesis.

Razan Sept. 18, 2019

Signature Date

ACKNOWLEDGEMENTS

I am grateful to be supervised by one of the most humanitarian professors: Dr. Ali Tehrani. His efforts were put to ensure the continuous development in the knowledge and skills of his students. He provided us a very supportive and motivating environment to enhance our research and educational expertise.

I would also like to thank Dr. Mohammad Ahmad, Dr. Kamel Abu Ghali, and Dr. Nisreen Ghaddar for their recommendations and assistance as being part of the thesis committee.

I want to tell my late father who once told me that he'd be dreaming about my future in a different world, that dreams seem to be permeable through the layers of both our worlds. As for the superwoman, my mom, who has overwhelmed me with love and care, none of this would have been possible without you. I also owe so much for my loving brother who was always there for me even in my midnight visits to the lab to turn on or off the electrospinning machine.

I express my utmost appreciation and thankfulness for my fiancé, Abdallah, who has probably heard the words "oil-water separation" and "surface modification" more than the words "I love you" during the past year, and yet managed to turn this experience to an unforgettable one.

I would also like to thank my lab partners, Ghadeer, Hadi, and Lamis, who would offer their help relentlessly.

Last but foremost, I thank God for all the blessings He has bestowed upon me.

AN ABSTRACT OF THE THESIS OF

Razan Ali Badran for Master of Engineering
Major: Chemical Engineering

Title: Surface Modification of the Electrospun Poly(vinyl chloride) Membrane for Oil-Water Separation

Oil pollution is a critical problem that is caused by the activity of several industries and oil spills. It causes damage to the environment and human life. Thus, an effective and versatile technique is needed to treat the oily wastewater.

The objectives of this thesis were to make (a) a hydrophobic porous membrane for separation of oil from water, and (b) a hydrophilic porous membrane by surface modification to remove water from oily wastewater by gravity. A series of polyvinyl chloride (PVC) electrospun membranes with various pore sizes (2.5 – 0.8 μm) was fabricated. The electrospinning process parameters such as voltage, tip-to-collector distance, and polymer-solvent ratio were optimized by Response Surface methodology to obtain a desired fiber diameter. The optimum conditions were found to be [polymer] = 16 wt%, the solvent ratio DMF:THF = 62.5:37.5, polymer feed rate = 1 ml/h, voltage = 11 kV, tip to collector distance = 14 cm, and drum speed = 500 rpm. The porosity, pore size distribution, hydrostatic pressure head, and membrane thickness were controlled by adjusting the electrospinning time. The pore size decreased with the increase of electrospinning time while the membrane thickness and hydrostatic pressure head increased. The resulting electrospun PVC membranes were superhydrophobic/superoleophilic with water contact angle above 140 ^{o}. The chemical stability of the membrane against different conditions of pH and salinity

was studied. Moreover, the oil filtration efficiency of the hydrophobic porous PVC membrane was investigated as a function of pore size for two membranes with the average fiber diameter of around 118 and 470 nm. The diesel oil recovery values after 45 minutes for the membranes with the average pore size of 2.5 μm and 0.8 μm were 95% and 80%, respectively.

Hydrophilization of the PVC porous membranes was achieved by surface modification using two different approaches: (1) The membrane was first aminated with triethylenetetraamine (TETA) and then cationized with N-(3-chloro-2-hydroxypropyl) trimethylammonium chloride , and (2) The membrane was aminated with polyethylenimine (PEI). The resulting hydrophilic membranes showed oil contact angle under water above 150^{o}. The separation efficiency of the modified membranes was tested using various oil and hydrocarbon types (diesel, toluene, decane, and cyclohexane). The electrospun PVC membranes showed very promising oil-water separation results with high efficiency of around 99.9%.

Keywords: Oil-water separation, nano-fibrous membranes, electrospun, surface modification, membrane.

CONTENTS

ILLUSTRATIONS

Figure Page

TABLES

Table Page

CHAPTER I

INTRODUCTION

Several industries generate oil-contaminated water during their operations. In the past years, the rapid industrial growth has led to massive production of oily wastewater, making it a global environmental concern. Oil spills in the seawater are the major source of oil pollution. In 2018 alone, the volume of oil spilled during oil transportation operations was reported to be 116,000 tons, a record in the last 24 years [1]. Other industries such as petrochemical, metallurgical, food and beverage, leather and textiles, automobile, and pharmaceutical, produce daily up to 140,000 L of oily wastewater per operation [2]. The produced oil differs in content (heavy and light hydrocarbons, fats, and oil and grease…), concentration (50-6000 mg/L), and form (free oil, dispersed, emulsified, and dissolved) [3]. The presence of the oil in these various states imposes a significant challenge on the industries. On the one hand, the wide bioavailability of the oil is threatening the whole ecosystem including but not limited to marine animals, plant growth, human health, and the environment [3]. On the other hand, they have to abide by the environmental regulatory limits in case of water discharge, and the specific operational limits in case of water reuse or recycle [4]. Thus, the need for a treatment technique that is efficient, cost-effective, environmentally friendly, and encompasses the versatility of the industries' treatment objectives becomes crucial.

There are various conventional techniques for treating oily wastewater based on physical, chemical, and biological processes. These techniques, although present some

advantages, still suffer from numerous drawbacks when it comes to the influent quality, separation efficiency, treatment cost, environmental footprint, and energy consumption. For example, API separators are only suitable for separating free oil with large oil droplets. Electrocoagulation releases metals in the effluent, and biodegradation is very sensitive to the environmental changes. Moreover, Pyrolysis requires high capital, maintenance, and operating cost. Electrochemical oxidation consumes large amounts of energy [5] [6]. Thus, the demand for a flexible and highly efficient technique that is able to respond to the industrial treatment objectives in separating the oil phase or the water phase arises. Membrane technology has emerged as a competent technique for the treatment of oily-wastewater [5]. It has many advantages such as its ability to separate oil in all its forms along with the other organic contaminants, its capability for functionalization and modification, and its relatively low cost and minimal environmental footprint [7]. The separation efficiency of a membrane is dependent on the membrane's structural and compositional properties, such as its roughness, fiber diameter, porosity, wettability, and surface tension [8]. Thus, the polymer used and the fabrication method are vital elements in determining the membrane's properties.

In order to produce an "oil-removing" membrane, several hydrophobic polymers have been investigated. Compared to other polymers, poly (vinyl chloride) presents several advantages for oil-water separation. Its hydrophobicity, excellent chemical stability, recoverability, and good compatibility with many polymers makes it an excellent candidate [9]. In terms of membrane fabrication, electrospinning has been employed as a robust method to produce nano-fibrous membranes with controllable morphology, high volume to the surface area, and high porosity, and rough hierarchical structure [10]. To enhance the

separation efficiency of the membrane, the electrospinning process and solution parameters (voltage, tip-to-collector distance, flow rate, solvent ratio, polymer concentration, and electrospinning time) have to be optimized to increase the membrane's permeability and separation flux. Response surface methodology is an optimization tool that investigates the effect of individual parameters and their interactions with each other on a certain process [11]. It is implemented to study the influence of the fabrication variables on the membrane's structure. However, the oil-removing membrane is prone to be easily fouled, blocked, and damaged by permeating oil. This disadvantage leads to a decrease in the separation efficiency and membrane's reusability [12]. In an attempt to overcome this issue, the wettability of the membrane is altered rendering it hydrophilic and underwater oleophobic. This may be achieved by several methods, such as surface modification, polymer grafting, and blending with additives and inorganic nanoparticles [23]. The currently available methods to fabricate hydrophilic and underwater oleophobic membranes requires rigorous procedures. In order to treat diverse wastewater solutions, several membranes are needed each made from a different polymer and fabricated by a different technique. Hence, there is an enormous demand to fabricate a highly efficient and durable water-removing membrane that has the capability of turning to an oil-removing membrane by a simple and easy modification.

In this thesis, the aim is to manufacture a membrane with dual functionality: oil-removing and water-removing, to increase the usability of the membrane and tailor its properties according to the wastewater solution's composition. The oil-removing membrane is fabricated by electrospinning PVC and optimizing its structure by investigating the effect of the process parameters using response surface methodology (RSM). Then, two novel

surface modification approaches are implemented. The first is based on quaternizing the PVC surface using the quaternary compound Quat-188. The second is based on functionalizing the PVC chain with amino groups using polyethylenimine (PEI). The separation efficiency of the original and modified membranes is studied using different oils and under various environmental conditions of pH and salinity.

CHAPTER II

LITERATURE REVIEW

A. Oily Wastewater Crisis

With industrial development, there is a tremendous increase in the consumption of oil, which is directly correlated to the rapid growth in oil pollution. The oily wastewater produced has become a crucial concern since it imposes significant threats to the soil, water, air, animals, and human beings. In this section, the different sources of oily wastewater and its hazards will be discussed.

1. Sources of Oily Wastewater

The primary source of oily wastewater is oil spills in the seawater. In 2018 alone, the volume of oil spilled was reported to be 116,000 tons, the largest record in the past 24 years [1]. Figure 1 shows an oil spill in the Gulf of Mexico. The secondary source is the industrial activities in the petrochemical, metallurgical, food and beverage, leather and textiles, automobile, and pharmaceutical sectors [13]. The tertiary source is a municipal waste. The generated oil from these various sources varies in type, concentration, and physical form. The wastewater may consist of heavy and light hydrocarbons, fats, oil and grease, lubricating oil, tars, wax oils, and cutting oil [3]. The concentration of each in the wastewater depends highly on its source. For example, petroleum industries generate large amounts of oil during field exploitation, oil extraction, and oil refining such that the concentration of oil and grease may reach to 4000-6000 mg/L. Metal processing industries

use high amounts of oil as well in grinding, cutting, lubricating, and cooling processes such that the generated wastewater contains oil of concentration that may reach up to 5000 mg/L. Moreover, food processing and packaging industries produce oily wastewater of oil concentration up to 1000 mg/L during slaughtering, cleaning, and producing vegetable and animal products. The lowest contribution of oil and grease content comes from domestic wastewater, where the concentration ranges between 50-100 mg/L [3].

The physical properties of the released oil such as its relative density, viscosity, volatility, and flow point, dictates its behavior in the water. Accordingly, a large amount of the oil exists in its free form and floats on the surface, part of it disperses or turns into emulsions in case of turbulence in the water surface, and the light hydrocarbon compounds of the oil might dissolve in the water [14].

Figure 1 Oily wastewater from an oil spill in the Gulf of Mexico [15]

2. Hazards of Oily Wastewater

As mentioned earlier, the oil, once released into the environment, undergoes several physiochemical processes that increase its exposure and bioavailability. Thus, it becomes a hazard on the whole ecosystem. The oily wastewater contains toxic compounds that impose risks on marine animals, plant growth, human health, and the environment [16]. The oil discharge affects the environment on short and long terms. The layers of oil on the surface of water restricts sunlight penetration and the dissolution of oxygen. This could lead to long term alterations of the marine biological processes and reproduction, causing the destruction of the habitat. The propagation of the toxic compounds among the marine food subsequently affects the whole chain including but not limited to birds, marine animals, and humans. In severe cases this might lead to carcinogenic and mutagenic effects on human health [3]. Moreover, direct human contact with the oil-polluted water highly harms the skin and might lead to the development of skin tumors [3]. The polluted water also contaminates the drinking water and groundwater resources and affects crop production [14]. Besides, light and volatile compounds in the oil evaporate causing air pollution [16]. Thus, the damage caused by oil has a ripple effect that impacts the whole ecological community.

B. Oily Wastewater Treatment Methods

Oily wastewater is one of the major threats to the environment. This threat is aggravating with the industrial growth and the increase in oily wastewater production. Thus, the treatment of the wastewater becomes inevitable. On the one hand, the industries have to meet the environmental regulatory limits upon water discharge, which vary with countries. For example, the allowable oil and grease limit for treated water discharge offshore in Australia is 30 mg/L as a daily average and that of the United States is 42 mg/L [4]. On the

other hand, treating the oily wastewater permits the industries to reuse and recycle the water or the oil cutting down their costs on raw materials [14]. Thus, understanding the sources of the oily wastewater, the properties of the oil and its concentration, and the treatment objectives of the industry are crucial to developing the appropriate treatment method.

1. Conventional Treatment Techniques

Oil-water separation can be achieved by either physical, chemical, or biological processes [4]. Several conventional techniques have been adopted, such as gravity separators, skimmers, air floatation, coagulation, flocculation, demulsification, biological treatment, adsorption, chemical precipitation, and bioremediation [13]. However, each of these techniques is suitable for a specific application and a specific objective. The treatment techniques are basically assessed based on the influent water quality that they are capable of treating, the effluent quality after separation, the treatment cost, the energy consumption, and the environmental footprint.

Regarding the influent quality, API separators for example are only suitable for separating free oil with oil droplets larger than 150 μm, while flotation is suitable to separate micro dispersed light oil droplets in the range of 5-100 μm but is not fit for the separation of highly viscous oil [14]. As for the effluent quality, electrocoagulation for example removes oil and grease with high efficiency but releases metals in the water [5], while biodegradation is able to degrade even the oxygen content and chemical content along with the oil and grease but takes very long time and the bacteria is susceptible to environmental changes [6]. Regarding the financials, ultrasonic irradiation and incineration have high equipment cost while pyrolysis requires high capital, maintenance, and operating cost. Flotation, on the other

hand, is more cost-effective on small scales but becomes infeasible for large scale separations [5]. Moreover, some methods consume large amounts of energy such as electrocoagulation and electrochemical oxidation [6]. Knowing that the aim of the treatment is to minimize the threats on the environment, certain techniques produce secondary pollution and require the usage of toxic chemicals and additives such as surfactant EOR and oxidation [5].

In light of what has been presented, the main drawback of the conventional techniques is their specificity towards limited wastewater quality and oil type and concentrations. This shortcoming obliges industries to adopt several treatment stages and methods depending on the waste solutions produced to reach their target. This imposes additional costs, installations space, and complex procedures.

2. Membrane Technology

Considering the limitations of the conventional techniques, the need for a versatile and universal oily wastewater technique arises. Membrane technology has been emerging as a competent method to separate oil from wastewater [5]. It offers vital advantages. Membranes are able to separate oil in its different forms whether free [17], dissolved, or emulsified [18] with high removal efficiency and permeate quality. Moreover, they have the ability to reject compounds other than oil such as COD, BOD, TS, TDS and TSS providing treated water quality within the regulatory limits [5]. They do not require the usage of chemicals reducing the waste and environmental footprint. Also, they need no or minimal energy consumption [7]. They offer great flexibility and malleability for modification and tunability depending on the application. Membranes are traditionally used in water treatment and desalination and have proved their liability and effectiveness in industrial scale plants

[7]. Moreover, they have been implemented in food processing, pharmaceutical, petroleum, and leather industries [13]. Thus, by taking advantage of these properties, the aim is to fabricate a membrane with dual functionality able to separate the oil phase and the water phase depending on their quantity and volume.

a. Theory and Practice

Membranes are made of either ceramic or polymeric materials. Ceramic membranes have excellent thermal and chemical stability, are inert to contact with steam, solvents, and strong acids, and have a very long-anticipated lifetime. However, they have high operation cost and significant weight. They are mainly used for size exclusion rather than adsorption since modifying them for molecular affinity is very difficult [8]. Polymeric membranes are versatile where they can be modified for a selective highly efficient separation. A wide variety of polymers can be used for different applications, each with specific affinity and properties. Polymers have low cost and high stability, permeability, formability, and processability. Polymeric membranes may be fabricated from either pure polymers or blended polymers to enhance the functionality of the membrane [8].

The performance of a membrane is primarily dictated by its structural and surface properties. Structural properties can be described by pore size, porosity, pore distribution, and pore tortuosity. Surface properties refer to the charge, roughness, and wettability [8]. Thus, to fabricate polymeric membranes with selective wetting properties for enhanced separation, the structural and surface properties are to be manipulated.

In terms of structural properties, the pore geometry and fibrous structure of the membrane are mainly controlled by the fabrication technique employed and polymer used.

The basic geometry of the membrane is denoted by parallel cylindrical pores perpendicular to the membrane surface where the pore length is equivalent to the thickness of the membrane. For such a geometry, the Hagen-Poiseuille equation describes the influence of the structural properties of the membrane on the permeate flux as follows:

$$J = \frac{\varepsilon r^2}{8\eta\tau}\frac{\Delta P}{\Delta x} \quad \text{(Eq. 1)}$$

where J is the flux, ε is the surface porosity, r is the pore radius, ΔP is the pressure difference across the membrane thickness Δx, η is the viscosity of the solution, and τ is the pore tortuosity [19].

For more complex geometries, the irregularities in the shape of pores and tortuosity, are accounted for in Kozney-Carman flux equation as follows:

$$J = \frac{\varepsilon^3}{K\eta S^2(1-\varepsilon)^2}\frac{\Delta P}{\Delta x} \quad \text{(Eq. 2)}$$

where ε is the volume fraction of pores, K is the Kozney-Carman constant that depends on the pore shape and tortuosity, and S is the internal surface area of the pores [19].

In terms of surface properties, the separation membranes are classified as either oil-removing or water-removing. Oil-removing membranes allow the passage of oil and repel the penetration of water. Membranes with water contact angle (WCA) higher than 90^o are considered to be hydrophobic and with WCA higher than 150^o are said to be superhydrophobic [13]. The development of a superhydrophobic membrane requires the incorporation of materials with low surface energy and rough topography [20]. Water-removing membrane is a membrane that allows the passage of water and repels the

penetration of oil. Membranes with water contact angle less than 90° are classified as hydrophilic. However, there is not a clear definition of a superhydrophilic membrane [20]. A schematic representation of the liquid-solid contact angles is shown in Figure 2.

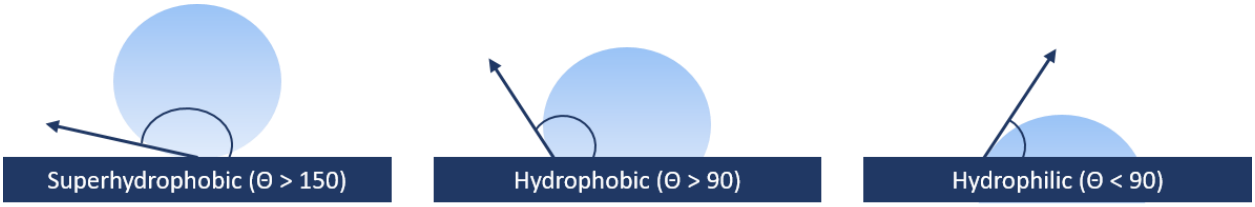

Figure 2 Contact Angles Schematic

The calculation of the contact angle of wetting is done using the Young-Laplace equation (Equation 3-a) [21]. It describes the balance sustained at the three-phase interface of solid, liquid, and vapor.

$$\gamma_{sv} = \gamma_{sl} + \gamma_{lv} cos\theta_Y \quad \text{(Eq. 3-a)}$$

where Υ_{sv}, Υ_{sl}, and Υ_{lv} are the interfacial tensions between the solid and gas phases, solid and liquid phases, and liquid and gas phases, respectively. Cos θ_Y is the equilibrium contact angle of wetting, also referred to as Young contact angle. The Young equation is developed on the assumption that the surface is topographically smooth and chemically homogeneous [21]. If the equation is extended to a liquid droplet on a solid surface in another liquid, the three-phase system equation is described by a modified Young's equation (Equation 3-b) as follows [22]:

$$\cos\theta_{ow} = \frac{\gamma_{oa} cos\theta_o - \gamma_{wa} cos\theta_w}{\gamma_{ow}} \quad \text{(Eq. 3-b)}$$

Where γ_{oa}, γ_{wa}, and γ_{ow} are the oil-air interfacial tension, water-air interfacial tension, and oil-water interfacial tension, respectively. θ_o, θ_w, and θ_{ow} are the contact angles of oil in air, water in air, and oil in water, respectively.

As for the relationship between roughness and wettability, Wenzel stated that increasing the surface roughness enhances the wettability of the surface. He described this phenomenon by the following equation – Wenzel Equation (Equation 4) [21]:

$$cos\theta_m = rcos\theta_Y \text{ (Eq. 4)}$$

where θ_m is the measured contact angle, θ_Y is the Young contact angle, and r is the roughness ratio (the ratio between the actual and projected solid surface area). The Wenzel equation applies under the assumptions that the droplet is higher than the roughness scale by two to three times and that the complete wetting of a rough surface occurs where the liquid penetrates the grooves of the surface [21]. In the case where these assumptions do not apply, the Cassie-Baxter equation is used. It assumes that vapor pockets are trapped beneath the liquid on the grooves resulting in two interfaces, solid-liquid and liquid-vapor. The Cassie-Baxter equation (Equation 5) is written as follows [21]:

$$cos\theta_m = f_s cos\theta_s + f_v cos\theta_v \text{ (Eq. 5)}$$

where f_s and f_v are the area fractions of solid and vapor on the surface. The figure below (Figure 3) schematically represents the mentioned theories [21].

Figure 3 (A) Young, (B) Wenzel, (C) Cassie-Baxter theoretical representations for the droplet wetting behavior on smooth and rough surfaces.

b. Oil-removing and Water-removing Membranes

As mentioned earlier, the oily wastewater quality and concentration vary between industries, and thus the permeate of interest, whether the water phase or the oil phase, varies as well. For example, petroleum industries are concerned with recycling the water phase to reinject it in the wells, reducing their costs. However, metal industries are interested in the oil phase to reuse it for lubrication and waxing [14]. Accordingly, there is a need for both oil-removing and water-removing membranes depending on the phase to be treated.

Oil removing membranes have gained significant attention since they have high separation efficiency, they are easy to handle, and they do not require the use of harmful chemicals [5]. However, hydrophobic/oleophilic membranes (oil-removing) have two main drawbacks. First, since water is denser than oil, it forms a layer on top of the membrane during separation hindering the process. Thus, separation by gravity alone is not possible, and the process requires external pressure and energy input. Second, these membranes can be easily fouled, blocked, and damaged by permeating oil [12]. This leads to a decrease in the membrane's separation capacity, reduces the recyclability of the membrane, and limits its practical applications [12]. Several techniques are employed to reduce the membrane fouling such as applying cleaning procedures, increasing turbulence in the membrane flow channels, and increasing the hydrophilicity of the membrane. Scientists were inspired by fish

scales that have underwater superoleophobic properties [22]. These surfaces, when immersed in water, repel oil and permit the penetration of water [23]. It was found that the superoleophobicity of a surface at water/solid interface is related to the hydrophilic nature of the surface at the air/solid interface [22]. This led to the emergence of superhydrophilic/underwater superoleophobic membranes. They have been used in a variety of applications such as preventing blockage, bio-adhesion, microfluidic technology, and oil-water separation [24]. Due to their remarkable properties, they have been investigated for oil-water separation. They enable the simultaneous separation of oil and water without any external energy input leading to a high separation efficiency [23]. Moreover, their resistance to oil fouling makes them easily recyclable and viable for large-scale oil/water separation [25].

Several approaches for the production of underwater superoleophobic membranes for oil-water separation have been reported in the literature such as surface modification, polymer grafting, and blending with additives and inorganic nanoparticles [26]. Yong et al. stated that the wettability of a surface is dependent on the geometrical microstructure and the chemical composition of the material. Thus, they aimed to produce a rough surface that has a hydrophilic nature. They fabricated a hierarchical micro/nanostructure silicon surface by a femtosecond laser. The laser-induced surface showed excellent properties where the oil contact angle reached up to 159.4^{o} and 150.3^{o} for 1.2-dichloroethane and chloroform, respectively [24]. Similarly, Dong et al. fabricated hierarchical polydimethylsiloxane (PDMS) surface upon introducing radical silanol group on the surface by oxygen plasma pretreatment [27]. Jin et al. grafted poly-(acrylic acid) to poly(vinylidene difluoride) filtration

membranes using a salt-induced phase-inversion approach leading to superhydrophilic underwater superoleophobic properties [26]. Gondal et al. spray deposited nanostructured TiO_2 on a stainless steel mesh substrate forming a mesh with 99% oil-water separation efficiency [28].

In summary, the currently available water-removing membranes lack durability and resistance to fouling. Moreover, the fabrication of hydrophilic and underwater oleophobic membranes requires rigorous procedures. In order to treat diverse wastewater solutions, several membranes are needed each made from a different polymer and fabricated by a different technique. Hence, there is an enormous demand to fabricate a highly efficient and durable water-removing membrane that has the capability of turning to an oil-removing membrane by a simple and easy modification.

C. Dual Functional Membrane Design

With the rising need for a highly efficient, durable, and cost-effective oily wastewater treatment method, a robust polymeric membrane is produced. The chosen polymer, fabrication technique, optimization of the fabrication parameters, and membrane surface modification will be investigated in this section.

1. The polymer of Study: Poly(vinyl chloride)

There is a substantial variety of polymers used for oil-water separation ranging between natural, synthetic, or a blend of both. The choice of polymer is dependent on its chemical, mechanical, and electrical properties such as high chemical resistance, high tensile strength, and high conductivity. Polyvinyl chloride (PVC) is the third widely used polymer such that its global production volume is 25 million tons per year [29]. The chemical structure

of PVC and some of its physical properties are shown in Figure 4 and Table 1, respectively. PVC has desirable properties for oil-water separation. It has excellent chemical stability, recoverability, hydrophobicity, and good compatibility with many polymers [9].

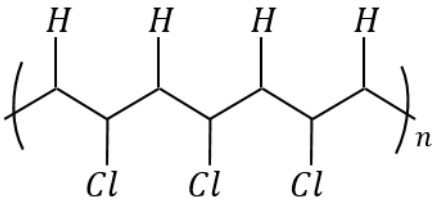

Figure 4 Chemical Structure of Poly(vinyl chloride)

Table 1 Physical Properties of Poly(vinyl chloride)

Physical Properties	**Value**	**References**
Chemical Formula	$(CH_2CHCl)_n$	[30]
Density	1.4 g/cm^3	[30]
Melting Point	160 - 300 ^oC	[31]
Glass Transition Temperature	80 - 100 ^oC	[31]
Thermal Coefficient of Expansion	54 - 110 e^{-6} (m/m K)	[32]
Inherent Viscosity	0.8 dL/g(lit.)	[30]

There are very limited studies on PVC membranes for oil-water separation application in literature. Ahmad et al. reported the fabrication of PVC ultrafiltration membranes using the phase inversion method. The membrane was used for separation of oil from wastewater produced from Digboi (Assam, India) oilfield with an oil concentration of 200 mg/L. The maximum obtained oil flux was 61.87 L/m^{2}h and oil rejection in the range of

91 – 92.5 % [33]. Su et al. developed a polyvinyl chloride/chlorinated polyvinyl chloride (PVC/CPVC) blend membrane using solvent-induced phase separation method for oil/water emulsion separation. The maximum permeate flux obtained was 43 $L/m^2/h$ with a rejection of 99.3 – 99.6% [34]. Moreover, Khan et al. produced polyvinyl chloride membrane using the electrospinning technique. The nanofibrous membrane was used to treat wastewater taken from the Tabuk Sewage Treatment plant in Saudi Arabia. The membrane showed 100% removal of oil and grease from the solution with an initial concentration of 4 mg/L [35]. However, there are still many gaps in studying the potential of PVC in oil-water separation and its performance in various environmental conditions.

2. Fabrication Method: Electrospinning

Various techniques are used to produce nanofibers such as drawing, template synthesis, melt-blowing, nanolithography, phase separation, self-assembly, and electrospinning. The attractiveness of these techniques varies according to the polymer types used, attainable fibrous structure, rate of production, and cost of production [36]. Electrospinning has emerged as a versatile and robust technique to produce fibers of controllable morphology with a vast range of polymers. This is a promising fabrication method for production of lightweight nano-fibrous membranes with high volume to surface area and high porosity [10]. It allows the design of fibers with diameters in the nano- to micro- range [11]. The distinctive properties of electrospun structures made them excellent candidates in areas such as drug delivery, tissue scaffolding, textiles, cosmetics, separation and filtration, and sensors [37].

Electrospinning is a dry spinning process by which an electrical field induced by a high voltage power supply is applied to the polymeric solution as shown in Figure 5 [38]. When the electric forces overcome the polymer solution surface tension, the thin jet is ejected from the tip of the needle in the form of a "taylor cone." During its trajectory, the charged jet is stretched and elongated and deformed into a spiral shape as the solvent evaporates. Polymeric fibers are deposited on the collector forming the resultant interconnected porous structure [10].

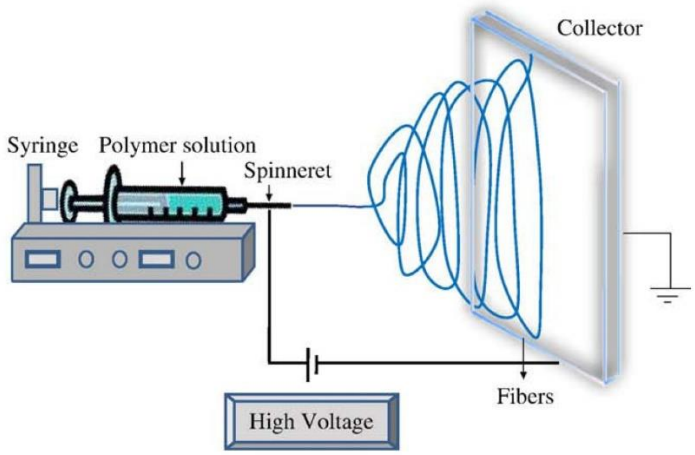

Figure 5 Electrospinning Process

The fibers morphology and orientation are dictated mainly by a set of solution, operation, and ambient conditions [10]. The properties of the polymeric solution such as the molecular weight, viscosity, surface tension, dielectric constant, conductivity, solvent volatility, solvent ratio, and polymer concentration have a significant effect on the produced fibers. A polymer with very high viscosity, low conductivity, and high surface tension would require high forces to form fibers and might lead to polymer solidification as the solution exits the needle [36]. Moreover, a solvent with low volatility would take time to evaporate

and cause wet fiber formation. Similarly, the operating conditions such as voltage, tip-to-collector distance, feed rate, collector rotation speed, and orifice diameter control the morphology of the fibers. Their effect is highly dependent on the polymer properties and each other [36]. For example, a polymer of low surface tension requires low voltage to form a stable jet. However, this stability is also dependent on the tip-to-collector distance. In addition, the surrounding conditions of humidity, temperature, and pressure also affects the solvent evaporation and thus pores formation [10].

Several electrospinning conditions have been reported in the literature to produce polyvinyl chloride bead-free fibers, as shown in Table 2.

Table 2 Electrospinning Conditions of PVC mats

Polymer	ES parameters	FD	References
PVC Solvent: DMF-THF	[polymer] = 10-15 wt% DMF:THF = 0:1, 80:20, 1:1, 20:80, 1:0 V = 8-15 kV TCD = 6 – 15 cm	200 nm – 6 μm depending on the parameters used	[39]
PVC Solvent: DMF-THF	[polymer] = 10 w/v% DMF:THF = 70:30 V = 10 kV TCD = 15cm F = 3 ml/h	400 – 800 nm	[40]
PVC Solvent: DMF-THF	[polymer] = 11 wt% DMF:THF = 1:1 V = 15 kV TCD = 24.5 cm F = 0.05 ml/min	340 ± 150 nm	[41]
PVC Solvent: DMF, THF, DMAc	[polymer] = 5–20 wt% V = 12 kV TCD = 15 cm F = 0.5 ml/h	For 20wt% concentration, FD is 1.63 μm, 1.35 μm, and 2.83 μm upon using DMF, DMAc, and THF as solvents, respectively.	[42]
PVC Solvent: DMF-THF	[polymer]= 12–16 wt% DMF:THF = 1:1 V = 20 kV	121 – 275 nm	[43]

	TCD = 20 cm		
PVC Solvent: DMF	[polymer] = 10 wt% V = 15 kV TCD = 20 cm F = 0.8 ml/h Rot speed = 200 r/min		[44]
PVC/PS Solvent: DMF-THF	PVC:PS = 10:90 wt% DMF:THF = 1:1 V = 25-30 Kv TCD = 15-20 cm	1.5 – 3 µm	[45]
PVC/natural rubber Solvent: THF	PVC:NR = 70:30 V = 16 kV TCD = 10 cm	PVC/LENR: 5-9 µm PVC/LENRA: 1-3 µm	[46]
PVC Solvent: DMF-DMAc	DMF:DMAc = 0.8:0.2 V = 25 kV TCD = 25 cm F = 2.5 ml/h	200 – 500 nm	[47]
PVC Solvent: DMF	[polymer] = 15 wt% V = 20 kV TCD = 13 cm F = 2 ml/h	205 nm **Note**: Increase in fiber diameter with increase in concentration	[48]
PVC Solvent: DMF-THF	[polymer] = 20 wt% DMF:THF= 5:5 V = 27 kV TCD = 20 cm F = 3 ml/h	1.6 – 2.4 µm	[49]
PVC/PAN Solvent: DMF-THF	[polymer] = 15 wt% PVC:PAN = 4:6 DMF:THF = 7:3 V = 27 kV TCD = 20 cm F = 2 ml/h	1250 nm	[50]

The influence of each of the solution and process parameters on the morphology and strength of the fibers of PVC electrospun mats has been studied. Zhu et al. reported the effect of the solvent on the fibers structure and mechanical properties. It was shown that upon the usage of THF alone as a solvent, a wrinkly surface structure of fibers formed due to the fast solvent evaporation and insufficient stretching. When DMF was added to the THF solution,

it retarded the solvent evaporation due to its low volatility and high electric conductivity, and thus improved the stretching process. The resultant fibers morphology was hence enhanced. However, the fibers produced with DMF alone as a solvent had a bead-on-string structure and small diameters. The mechanical strength of the fibers produced with a mixed DMF/THF solution was the highest [40]. The mechanical strength of the fibers is highly dependent on their morphology. The presence of beads causes less fiber to fiber interactions and more weakness of individual fibers resulting in low tensile strength. Thus, bead-free smooth fibers possess increased tensile strength [43]. Similarly, Lee et al. reported that upon the usage of THF alone, the capillary tip was often closed due to its low boiling point. Moreover, a broad distribution of diameters was obtained, ranging between 500 nm to 6 μm. On the other hand, a narrow distribution of diameters was achieved upon the usage of DMF only with an average diameter of 200 nm. THF is an excellent solvent for PVC but has low dielectric properties while DMF is a poor solvent compared to THF with remarkable electrolyte behavior. Thus, the electrospun fibers with a mixed solvent solution of THF and DMF with solvent ratios of DMF:THF 60:40, 50:50, and 40:60 showed optimal morphology [39].

Zulfi et al. studied the effect of polymer concentration on the electrospinning process. They observed that there is a critical concentration of PVC solution after which the electrospun PVC underwent a morphological change from particles to fibers. This concentration is dependent on the solvent used as well. Upon the usage of DMF, DMAc, and THF, the critical concentrations were 10 wt%, 20 wt%, and 15 wt%, respectively [42]. Tarus et al. attributed this morphological change to a change in solution viscosity. The solution concentration dictates the polymer chain molecules entanglement within a solution which

determines the solution viscosity. During electrospinning, a solution with low viscosity causes the jet to partially break up due to its inability to match the electrostatic and columbic repulsion forces. Influenced by surface tension, the high number of free solvent molecules in the solution group in a spherical shape forming beads. Upon the increase in polymer concentration, the viscosity of the solution increases with the increase in polymer chain entanglements. Thus, the viscoelastic solution force is enhanced, preventing the partial breakup of the jet. Moreover, the solvent molecules are able to be distributed over the entangled polymer molecules leading to the formation of smooth fibers and enhanced fiber uniformity [43].

In addition, the effect of PVC molecular weight was studied by Zhu et al. Two solutions with varying molecular weights of M_w 6.65×10^4 g/mol and 8.83×10^4 g/mol were electrospun. It was found that as the molecular weight of PVC increased, the bead-on-string fibers disappeared [40].

Lee et al. also reported the influence of applied voltage and tip-to-collector distance on the structure of the fibers. They reported that the fiber diameter decreased with an increase in voltage from 8 to 15 kV and an increase in tip-to-collector distance from 6 to 15 cm [39].

Subsequently, other studies have been carried out to gain a deeper understanding of the influence of the parameters governing the electrospinning process on the fiber formation. The control of these parameters is necessary to achieve specific functionalities of the electrospun fibrous networks. For instance, strong and durable membranes are required for applications such as filtration and protective fabrics, and stiff membranes are needed for applications such as tissue engineering [37]. Comprehensive quantitative studies are needed

to determine the correlations between the different parameters and their effect on fiber diameter, porosity, mechanical strength, and permeability. Conventional studies use a systematic approach that tests the impact of one factor at a time, keeping the other parameters constant. This method fails to take the interactive relations between the different parameters into account and is very time-consuming. Thus, it provides an incomplete framework to control the morphology of the fibers preventing the usage of the electrospun nanofibers to their full potential [51]. Some researchers conducted a regression analysis to obtain equations that relate the electrospinning parameters to the desired outcome in an attempt to fine-tune the electrospinning process [43].

However, these equations only present specific relations between two factors and are not inclusive to the overall interactions. These shortcomings can be overcome by using novel optimization methods that establish a quantitative relationship between the electrospinning parameters and the desired outcome.

3. Optimization of Membrane Properties: Response Surface Methodology

Response surface methodology (RSM) is an optimization tool that investigates the effect of individual parameters and their interactions with each other on a certain process [11]. It is a combination of mathematical and statistical methods used to optimize, model, and analyze the performance of the variables affecting the response of interest [37]. It generates a mathematical model that conveys the relationship between the parameters as given in Equation 6[52]:

$$\eta = f(x_1 . x_2 . \ldots . x_n) + \varepsilon \quad \text{(Eq. 6)}$$

where η is the response, f is the function of response, x_1, x_2,…, x_n are the process variables, n indicates the number of variables, and ε refers to the statistical error that is caused by the other sources of variability not accounted for by f.

The optimization study using RSM can be divided into three stages. In the first stage, a preliminary study is performed to determine the independent variables affecting the process and their levels. In the second stage, the experimental design is selected, and the model equation is then generated and verified. In the third stage, the optimum design is determined, and the response surface plots and contour plots showing the influence of the independent parameters on the response are obtained [52].

In the first stage, screening experiments are performed to determine the parameters that have primary effects on the process. Usually, many variables influence the response of interest, but accounting for them all would be very effort and time-consuming. Then, after the identification of the main parameters, the levels of these parameters are to be chosen carefully in a way that would cover all the accessible range that would lead to successful optimization. Afterward, since the parameters have different units and/or operate in different ranges, they should be normalized to be able to perform a regression analysis. Thus, each coded variable is forced to range from -1 to 1 by using the following coding and normalization equation (Equation 7). In this way, all the parameters influence the response more evenly, and their units become irrelevant.

$$X = \frac{x-[x_{max}+ x_{min}]/2}{[x_{max}- x_{min}]/2} \text{ (Eq. 7)}$$

where X is the coded variable, x is the natural variable, x_{min} and x_{max} are the minimum and maximum values of the natural variable, respectively [52].

In the second stage, the response surface design is chosen. RSM offers several designs that differ based on the number of experimental points, runs, and blocks. For experiments with parameters of two-levels only, factorial designs are used. They are very beneficial for screening experiments to identify the major parameters and to fit a first-order response surface model. For parameters with at least three levels, central composite design (CCD) and Box-Behnken design (BBD) are used. These designs possess the required properties to fit a second-order model described, as shown in Equation 8[53]:

$$y = \beta_o + \sum_{j=1}^{k} \beta_j X_j + \sum_{j=1}^{k} \beta_{jj} X_j^2 + \sum\sum_{i<j} \beta_{ij} X_i X_j + \varepsilon \quad \text{(Eq. 8)}$$

where β_o, β_i, β_{jj}, and β_{ij} are regression coefficients for intercept, linear, quadratic, and interaction coefficients respectively, X_i and X_j are the coded independent variables, and ε is the random error component.

The central composite design is used for sequential experimentation where it builds on previous factorial experiments to generate a full quadratic model. It can include up to 5 levels per factor. Box-Behnken design usually has fewer design points than the central composite design, which makes it more affordable to run with a similar number of factors. However, it cannot run from a factorial experiment, and it always has three levels per factor only. The Box-Behnken design ensures that all factors are within the safe operating zone while central composite design usually has axial points outside the region of interest which may be impossible to operate since they are beyond the safe operating limits [54].

In the third stage, response surface plots and contour plots are generated to visualize the predicted model equation. The response surface plot demonstrates the relationship between the response and the independent variables through a theoretical three-dimensional plot. The contour plot shows the shape of the response surface through a two-dimensional display of the surface plot [52].

4. Surface Modification: Two Novel Approaches

The aim of this project was to manufacture a membrane with dual functionality: oil-removing and water-removing, to increase the usability of the membrane and tailor its properties according to the wastewater solution's composition.

Although oil-water separation has been investigated extensively using lots of polymers, it has been challenging to produce a membrane using the low-cost PVC with enhanced properties and simple manufacturing procedures. The oil-water separation capability of the PVC as an "oil-removing" membrane has been very briefly investigated in literature [35]. In this work, the electrospun PVC membrane was optimally designed by manipulating the process and solution variables to produce a highly rough hierarchical nano-fibrous structure capable of separating the oil phase from the water phase with high efficiency. The separation characteristics of the membrane were comprehensively studied in regards to types of oils used, medium pH, and salinity.

The modification of PVC to alter its wettability to become hydrophilic has been achieved by adding polymer blends such as poly(vinyl butyral) [55], additives such as poly(vinyl pyrrolidone) [56], poly(ethylene glycol) [57], bentonite [58], and pluronic F127 [59], inorganic nanocomposites such as Fe_2O_3 [60], TiO_2 [61], ZnO [62]. However, the

mentioned fabrication methods focus on modifying the initial PVC solution before manufacturing rather than surface modifying the PVC mat after manufacturing. Moreover, they are complex and require multiple staged procedures. Note that, the fabrication of a hydrophilic/ underwater oleophobic PVC membrane has not been reported.

In our work, the fabricated PVC membrane was used for "water-removing" treatment applications, as well, upon introducing two novel surface treatment techniques. The first technique is based on cationizing the PVC membrane and the second is based on the functionalization of amino groups on the PVC surface.

In the first approach, the reaction of PVC with a cationizing agent leads to the functionalization of a quaternary ammonium group on the carbon chain with a positive charge and a highly hydrophilic wettability [63]. Moreover, the cationized membrane becomes pH-independent since the quaternary ammonium group is in the ionized form regardless of the pH of the medium [64]. The quaternization of PVC has been investigated very briefly to enhance its antibacterial effects. Palencia et al. chemically modified PVC by a reaction with dimethylamine followed by the quaternization using 1-bromoethane[65]. Wu et al. were the only group that reported the surface quaternization of the PVC membrane using trimethylamine (TMA) [66]. However, the water permeability was low. A new method is introduced to quaternize the surface of the PVC membrane that is based on the nucleophilic substitution and quaternization of amino groups using triethylenetratramine (TETA) and 3-chloro-2-hydroxypropyl trimethyl ammonium chloride (Quat-188), respectively.

TETA is a highly reactive primary aliphatic amine [67]. It is used as a modifying agent for dye removal [68], ultrafiltration [69], and heavy metal adsorption [70]. Quat-188 is

a positively charged quaternary ammonium reagent. It has been used to modify materials to enhance their capacity for adsorption of surfactants [64], antibacterial effects [71], self-cleaning performance [63], and dye fixation [72]. The proposed reaction does not require any complicated measures and

The second approach is the reaction of PVC with polyethyleneimine (PEI). PEI is a long-chain polymer that has primary, secondary, and tertiary amine groups [73]. It has been widely used to enhance the adsorption performance of adsorbents for the removal of dyes [74], heavy metals [75], and precious metals [76]. The reaction of PVC with PEI has been briefly reported in the literature for the removal of palladium Pd(II) [77], platinum Pt(IV) [73], and mercuric and cupric salts [78]. However, it has not been tested for oil-wastewater treatment applications. The modification method is a single-step reaction that leads to the functionalization of PVC with amino functional groups rendering the membrane hydrophilic and underwater oleophobic.

CHAPTER III

MATERIALS AND METHODS

A. Materials

Polyvinyl chloride (PVC) with a molecular weight of 80,000 g/mol and a density of 1.4 g/mL, dimethylformamide (DMF) with ≥ 99.8% purity, tetrahydrofuran (THF) with ≥ 99.9% purity, decane with ≥ 95% purity, cyclohexane with ≥ 99% purity, branched polyethylenimine with a molecular weight of M_w=25,000 by LS, and 3-Chloro-2-hydroxypropyl)trimethylammonium chloride solution (Quat-188) 60 wt% in H_2O were all purchased from Sigma. Commercial nylon screen fabric with an average pore size diameter of 350 µm and thickness of 215±2 µm was used as a support for the electrospun membranes. Galwick , a wetting solution with a surface tension of 15.9 mN/m, was purchased from Porous Material Inc., NY, USA. Commercially available diesel oil (density of 700 kg m^{-3} and a viscosity of 18.2 cP @23.7C) and vegetable oil (density of 930 kg m^{-3} and a viscosity of 49.84 cP @25.3 C), were used for oil-water separation experiments.

B. Electrospinning of Membranes

PVC was dissolved in a mixture of DMF and THF (62.5:37.5) by magnetic stirring at an apparent speed of 700 rpm and at room temperature. The solution was electrospun using a laboratory-scale electrospinning machine (FLUIDNATEK LE-10, BIOINICIA, Spain). The prepared solution was fed into the metal capillary nozzle using a syringe pump. A rotating cylindrical drum made of anodized aluminum (Diameter=0.1m and Length=0.2 m) was used to collect the nanofibers at apparent collecting speed (CS) of 500 rpm. The flow

rate was set at 1 ml/h. The conditions of temperature and humidity were maintained at 22 ± 2 ^{o}C and 50 ± 5%, respectively.

C. Design of Experiment

1. Screening the Parameters

In the first phase, the electrospinning parameters that have significant effects on the morphology of the fibers along with their levels were determined by screening (preliminary) experiments to be flow rate, solvent ratio, voltage, tip to collector distance, and polymer concentration [40, 42, 45]. The flow rate was optimized to fabricate the mesh within a desirable period of time. Thus, a flow rate of 1 ml/h was chosen. As for the solvent ratio, solutions of solvent ratios of DMF:THF 100:0, 80:20, 20:80, and 0:100 were not soluble for dissolving and were not adequate for electrospinning in terms of their viscosity, surface tension, and conductivity [39]. Thus, a solvent ratio of DMF:THF of 62.5:37.5 was chosen. Regarding the voltage, tip-to-collector distance, and polymer concentration, the ranges were chosen based on literature, and they were as follow: 11-17 kV, 11-17 cm, and 12-16 wt%, respectively.

2. Variables and Design Selection

According to the screening analysis, the main parameters that affect the morphology of the membranes are polymer concentration (wt%), voltage (kV), and tip-to-collector distance (cm). The solvent used is a mixture of DMF:THF with a ratio of 62.5:37.5, and the flow rate was set to 1 ml/hr. The levels of the parameters were chosen such that a stable jet was maintained. The selected design was Box-Behnken since it provides the best efficiency with the least number of experiments for three factors with three levels system. The factors

were normalized according to **Error! Reference source not found.** to range between -1 and 1 . The resultant coded and actual variables are presented in Table 3.

Table 3 Actual and coded values of the selected factors

	Coded Variables		
	-1	0	1
Polymer Concentration (wt%)	12	14	16
Voltage (kV)	11	14	17
Tip to collector distance (cm)	11	14	17

The statistical analysis of the experimental data, including the design, regression analysis, and data plots, was performed using Minitab® 18.1 Statistical Software.

D. Surface Modification of the Membrane

1. PVC Modification with Quat-188

The first step was reacting PVC with TETA. The TETA solution was prepared by dissolving TETA in ethanol in a ratio of 1:100 v/v. Then, the PVC membrane was immersed in the solution such that the ratio of PVC (g) to TETA (ml) is 1:1. The reaction was held at 65 ^{o}C for 4 hours. Afterwards, the membrane was washed with ethanol and water, and left to dry at room temperature.

The second step was reacting the TETA-modified PVC membrane with Quat-188. An aqueous solution of 60 wt% Quat-188 was used. The pH of the solution was adjusted to 8 using 1wt% NaOH solution. The ratio of PVC (g):Quat-188 (ml) was 1:100, and that of

NaOH solution (ml):Quat-188 (ml) was 1:1. The PVC membrane was introduced into the Quat-188 solution and placed in a water bath. The reaction temperature was raised gradually to 70 ^{o}C. Meanwhile, the NaOH solution was added in three batches every hour. The total reaction time was four hours. At the end of the reaction, the membrane was acidified with 1% acetic acid solution and then washed with distilled water. The membrane was then left to dry at room temperature.

2. PVC Modification with PEI

A solution of PEI in ethanol was prepared such that the weight ratio of PEI to PVC was 1:1. The solution ratio was 0.1g (PEI):10 ml (ethanol). The PVC membrane was introduced in the solution and placed in a water bath. The reaction was held at a temperature of 65 ^{o}C for four hours. Afterward, the membrane was washed with ethanol and left to dry at room temperature.

E. Membrane Characterization

1. Fiber Diameter Measurement

The fiber diameter of the membranes was measured using a Field Emission Scanning Electron Microscope (SEM, MIRA 3 LMU Tescan, Czech Republic). The membrane samples were placed in a sputtering coater (Q150 Quorum Technologies) to be coated with a thin layer of Gold. The coated sample was then introduced in the SEM vacuum chamber and fixed on the sample holder. An acceleration voltage of 5-20 kV is applied, and a SE Beam Detector is used. The average fiber diameter measurement is calculated based on at least 100 measurements.

2. Porosity, Pore Size and Hydrostatic Pressure Head (HPH) Measurement

The porosity of the membrane was determined using the following formula:

$$Porosity\ (\%) = 1 - \frac{\rho}{\rho^o} \text{ (Eq. 9)}$$

Where ρ is the bulk density of the membrane and ρ^o is the apparent density of the polymer [79]. The membrane density was calculated upon weighing a sample of known area (2cm × 2cm) and thickness.

The average pore size and HPH of the membranes were measured using a capillary flow porometer CFP-1100- from Porous Material Inc. (PMI), USA. In order to measure the average pore size, a membrane sample was horizontally sandwiched in the sample chamber, saturated with a wetting liquid, Galwick, then, properly sealed. Afterward, an inert gas, air, is passed into the chamber at an increasing differential pressure. When the pressure reaches an adequate level to overcome the capillary action of the fluid in the largest pore, the fluid is displaced in that pore. The corresponding pressure is the bubble point. The pressure is increased further until the liquid in all pores is displaced and the sample is considered dry. Meanwhile, the flow rate and gas pressure are monitored in order to generate the pore size distribution and mean pore size diameter.

Laplace equation describes the pressure required to eliminate the liquid from the pores of the membrane [80]:

$$\Delta P = \frac{4\gamma cos\theta}{D} \times \beta \text{ (Eq. 10)}$$

Where ΔP is the pressure required to displace the liquid in the pore, γ is the surface tension, θ is the contact angle, D is the pore diameter, and β is the correction factor (0.715).

The hydrostatic pressure head corresponds to the maximum height of water the membrane can withstand before it leaks. In order to measure the HPH, the membrane is similarly sandwiched in the sample chamber and it is covered with a layer of water. The air pressure is increased gradually until the first droplet of water leaks through the membrane. This pressure is reported as the HPH.

3. Contact Angle Measurement

The contact angles of water (WCA) and oil (OCA) were measured using an optical tensiometer (OCA 15EC, DataPhysics, Germany) with a droplet volume of 5 μm. The underwater OCA was measured by placing an oil droplet of volume 5 μm in contact with the membrane from the bottom while immersed in water. The measurements were repeated for a minimum of 20 times for each sample.

4. Membrane Properties

Fourier transform infrared spectroscopy (Agilent Technologies Cary 630 FTIR) was used to characterize the chemical composition of the nanofibrous membranes, and the Agilent MicroLab PC software was used to display and evaluate the results.

Thermogravimetric Analyzer (TGA) (TGA Q500, TA Instruments) was used to conduct a thermogravimetric analysis for the samples. All the samples were heated to 800 °C at a linear heating rate of 10 °C min^{-1} under dynamic nitrogen flow.

Differential Scanning Calorimetry (DSC) (Q2000 Differential Scanning Calorimeter, TA Instruments) was used to study the behavior of the membranes as a function of temperature. The samples were introduced in Tzero Aluminum Hermetic pans. They were

exposed to a series of heating/cooling/heating cycles. The temperature was raised from 25 ^{o}C to 120 ^{o}C and back to 25 ^{o}C at a rate of 10 K/min.

Particle Size Analyzer (90 Plus/BI-MAS, Brookhaven Instruments Corporation, USA) was used to detect the oil content in the separated water and the water content in the separated oil.

F. Oil-Water Separation Setup

The oil-water separation was conducted using a pressure-driven filtration setup for the oil-removing membrane and a gravity-driven filtration setup for the water-removing membrane. The pressure-driven filtration setup was designed for batch separation processes. Figure 6 shows a schematic representation of the process and the actual lab setup. It consists of a laboratory-scale cell membrane holder (CF042-FO, Sterlitech Co.) with an effective membrane area of 0.0042 m^2 and two inlets and two outlets. The mixture of oil and water was pumped at a speed of 70 rpm through one inlet using a peristaltic pump (Masterflex model 77200-62, Longer Pump Co.). Afterward, the filtrate was directed back to the beaker containing the mixture of oil and water and the separated oil was collected in a beaker placed on a balance (GX-30K high capacity balance, A&D). The weighing data were retrieved from the balance using WinCT© software application and displayed in graph form on the monitor screen in real-time using RsWeight tool.

As for the gravity-driven filtration, the membrane was fixed between two glass funnels with an effective separation area of 1.26×10^{-3} m^2. The mixture of oil and water was poured into the upper glass funnel, and the separation was achieved through the membrane.

The separated liquid was collected in a beaker placed on the balance, where the weighing data was retrieved as well using the WinCT software.

The volume of liquid recovered through the membrane was calculated from the following Equation 11:

$$Volume\ of\ liquid\ recovered\ \left({ml}/{m^2}\right) = \frac{m/\rho}{A} \quad \text{(Eq. 11)}$$

Where m (g) is the weight of the filtrated liquid, ρ (g/ml) is the density of the filtrated liquid, and A (m^2) is the effective surface area of the separation membrane in the setup.

The separation efficiency (η) of the liquid through the membrane was obtained through the following Equation 12:

$$\eta\ (\%) = \frac{V_{after}}{V_o} \times 100 \qquad \text{(Eq. 12)}$$

Where V_o and V_{after} are the volumes of the separated liquid before and after the separation, respectively.

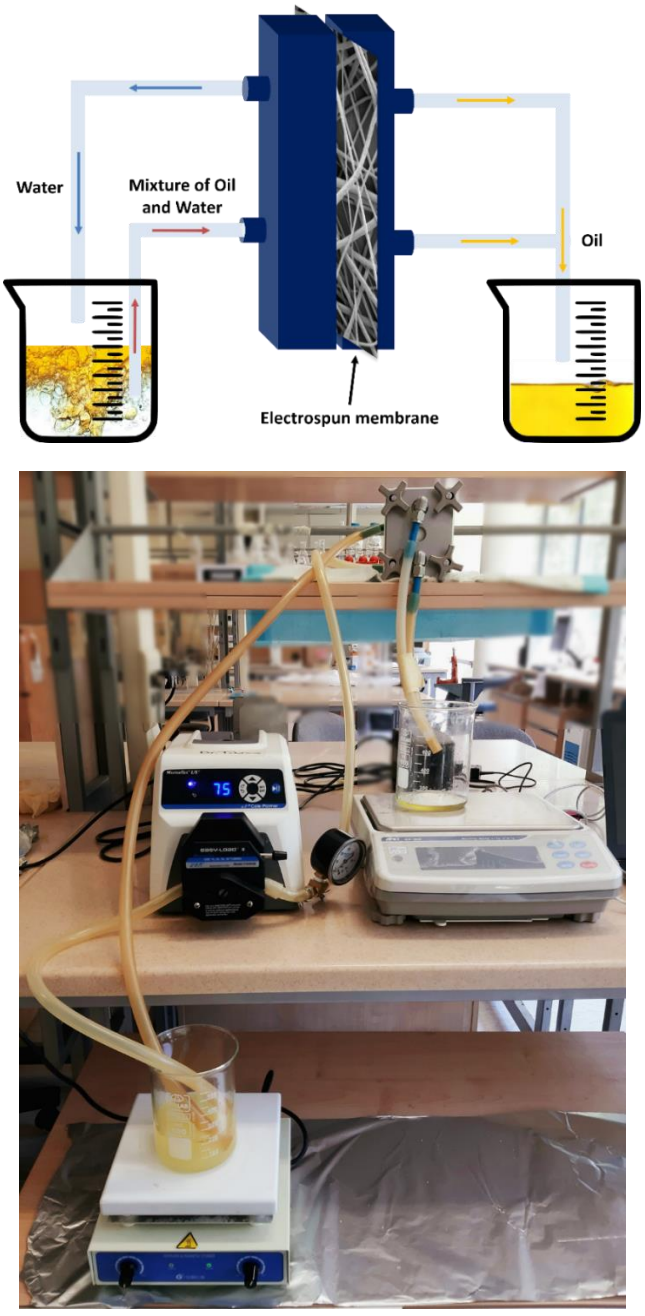

Figure 6 Pressure-Driven Oil-Water Separation (a) Schematic Setup and (b) actual lab setup

CHAPTER IV

RESULTS AND DISCUSSION

A. Optimization of the Electrospinning Parameters

Electrospinning is a very promising technique in producing nanofibers with diameters in the submicron to nanometer range. The electrospinning of PVC was successfully achieved by producing bead-free fibers for the chosen ranges of parameters. Figure 7 displays the SEM image of one sample of the PVC electrospun membranes showing smooth and beads-free nanofibers. The nanofibers are randomly distributed and stacked layer above another.

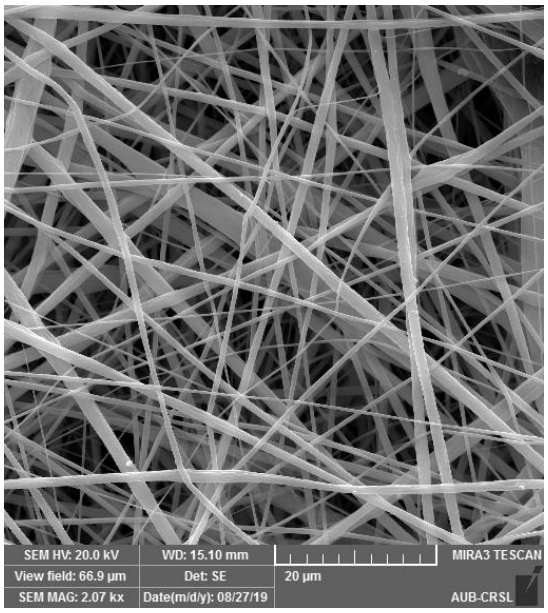

Figure 7. SEM Image of the electrospun PVC membrane

The electrospinning parameters were optimized to control the various parameters affecting the performance of the electrospun membrane (e.g., fiber diameter, pore size, hydrostatic pressure head, and thickness) to achieve the highest oil-water separation efficiency. Thus, initially the effect of the parameters on the fiber diameter was studied. Afterward, the thickness, pore size, and hydrostatic pressure head were adjusted by changing the electrospinning time.

1. Effect of Electrospinning Parameters on Nanofibers Diameter

In this study, the effect of various process and solution parameters (polymer concentration (wt%), voltage (kV), and tip-to-collector distance (cm)) on the diameters of the fibers was studied. The fiber diameter of every sample was obtained by averaging 100 measurements from the SEM images as shown in Figure 8. The confidence intervals were obtained within 95% confidence level.

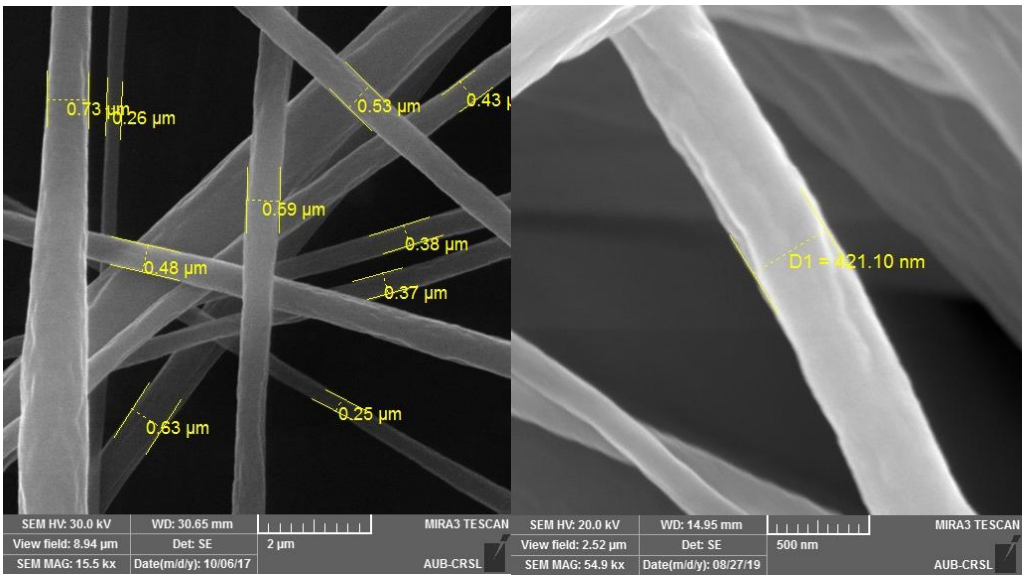

Figure 8 SEM Images of Electrospun PVC Membrane with sample fiber diameter measurements (a) over a section and (b) over a representative fiber

Table 4 depicts the Box-Behnken design and the results of the experiments. These results are modeled in Figure 9 by contour and 3D surface plots.

Table 4 Box-Behnken Design and Experimental Response

RunOrder	Blocks	PVC wt%	Voltage (kV)	TCD (cm)	FD (nm)	Standard Deviation	Confidence Interval
1	1	-1	-1	0	158	61	0.38
2	1	0	0	0	241	84	0.53
3	1	-1	0	-1	118	36	0.23
4	1	0	0	0	242	131	0.83
5	1	1	0	1	480	251	1.58
6	1	-1	1	0	129	38	0.24
7	1	1	0	-1	436	173	1.09
8	1	0	-1	-1	352	158	0.99
9	1	0	0	0	316	132	0.83
10	1	0	1	-1	311	121	0.76
11	1	1	-1	0	354	227	1.42
12	1	0	-1	1	472	213	1.34
13	1	0	1	1	272	107	0.68
14	1	1	1	0	390	182	1.15
15	1	-1	0	1	162	46	0.29

Figure 9-a depicts the interaction between PVC polymer concentration and the applied voltage. The fiber diameter appears to be highly dependent on the polymer weight concentration, as it increases from 100 nm to 400 nm as the PVC wt% increases from 12 to 16 wt% with a constant voltage. On the other hand, the voltage seems to have a more pronounced effect at low polymer concentration than at high concentration leading to a decrease in the fiber diameter as it increases. The interplay between polymer concentration and voltage is crucial in the formation of fibers. There is a minimum concentration required for the formation of bead-free uniform fibers. At low concentrations, the viscosity of the solution is low, and thus the applied voltage and the surface tension lead to the breaking of the entangled polymer chains into fragments. The polymeric solution stretches as the electrostatic repulsive forces on the surface of the jet increase leading to the formation of thinner fibers. As the polymer concentration increases, the viscosity of the solution and the chain entanglements increase. These chain entanglements can overcome the effect of the voltage and surface tension leading to the formation of uniform electrospun nanofibers [81], [82]. Similar results were obtained upon the electrospinning of chitosan [83], poly(vinylidene fluoride) [84], and polyvinyl alcohol [85].

Figure 9-b reflects the interaction between the polymer concentration and the tip-to-collector distance. At low tip-to-collector distance values (11-14 cm), the fiber diameter decreases as the TCD increases. Beyond this value, the increase in TCD leads to an increase in the fiber diameter. This influence is more apparent in Figure 9-c, as the influence of TCD on the fibers morphology is relatively similar to that of voltage and less significant compared to that of PVC concentration. The tip-to-collector distance dictates the time till the fibers

deposit on the collector, the evaporation rate of the solvent, and the whipping or instability range. As the TCD increases, the fibers take enough time to dry before reaching the collector leading to thinner fibers [86]. However, beyond a certain limit, the influence of the electric field weakens, thus the fiber diameter increases [87].

Accordingly, the optimal parameters to obtain fibers with maximum diameter are PVC wt% of 16%, voltage of 11 kV, and tip-to-collector distance of 14 cm. On the other hand, the optimal parameters to obtain fibers with the lowest fiber diameter are PVC wt% of 12%, voltage of 17 kV, and tip-to-collector distance of 17 cm. The results are shown in the optimization plots in Figure 10.

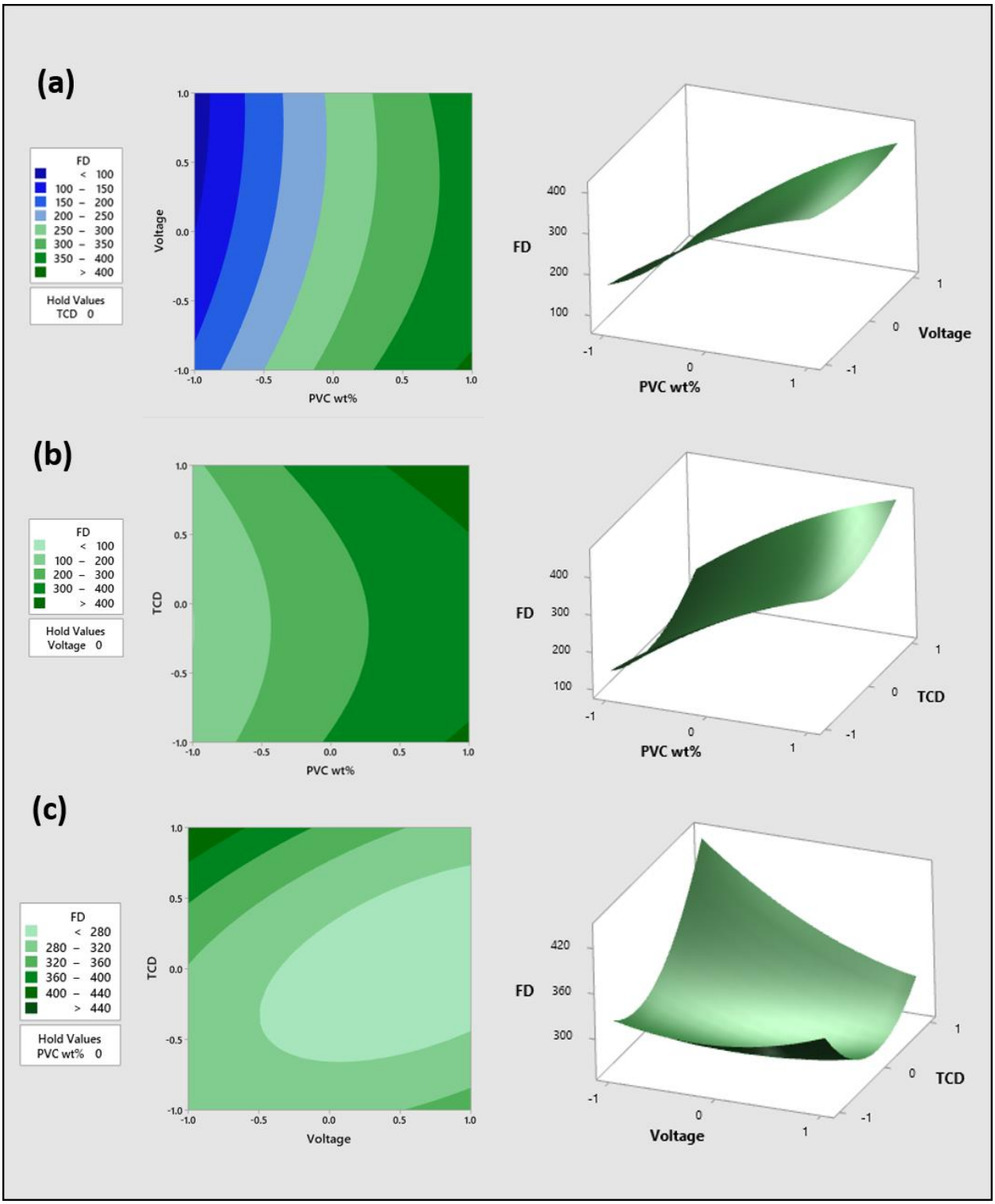

Figure 9 Contour and three-dimensional response surface plots as a function of: (a) applied voltage and PVC concentration (b) tip to collector distance and PVC concentration (c) tip to collector distance and applied voltage.

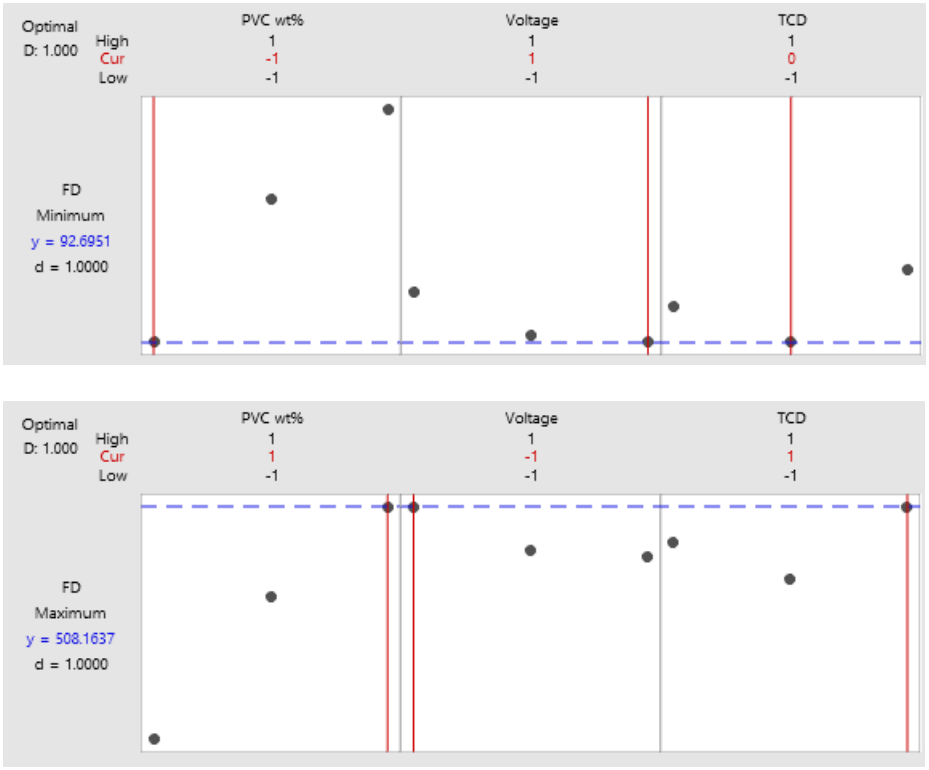

Figure 10 Optimization Plot for target fiber diameter (a) minimum and (b) maximum

2. *Effect of Electrospinning Time on Thickness, Pore Size, and Hydrostatic Pressure Head*

The influence of the electrospinning time on the thickness of the membrane was studied. Figure 11 showed that the thickness of the membrane increased almost linearly with time as more fibers were deposited on the collector. These fibers formed an intertwining structure, stacking a layer above another, and obstructing the already existing pores. This led to a decrease in the pore size that is observed in Figure 12. Moreover, as the pore size decreased, the pressure required to cause leakage of water through the pores increased according to Laplace equation (Equation 10).

Thus, the hydrostatic pressure head increased as shown in Figure 12. In addition, it is observed that the increase in the fiber diameter from 118 nm to 470 nm led to an increase in the pore size from a range of 2.5 – 1.5 µm to 1.2 – 0.8 µm, respectively. Table 5 summarizes the properties of the electrospun membranes.

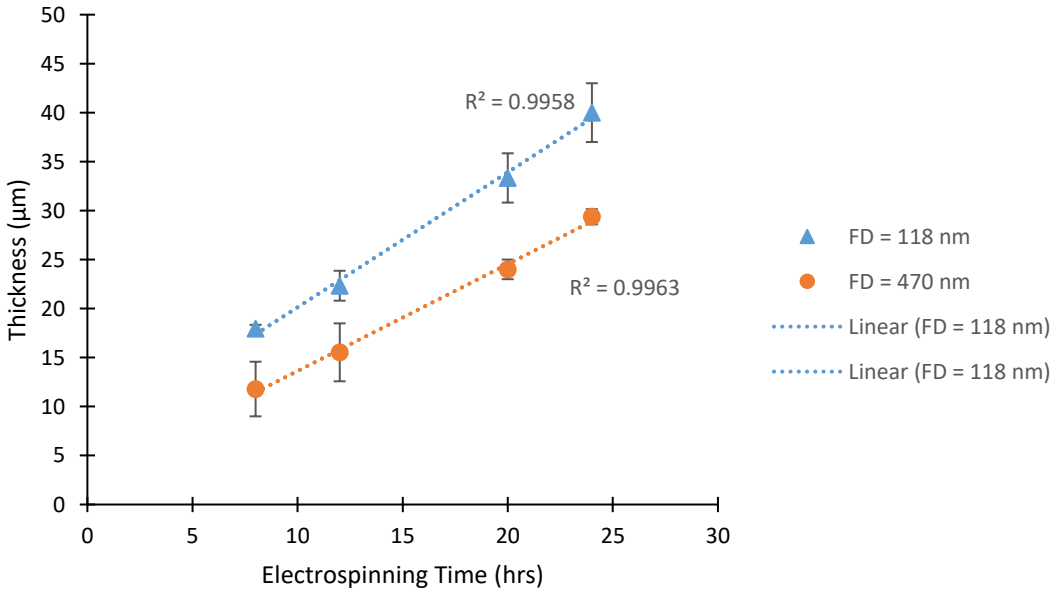

Figure 11. Effect of time of electrospinning on the membrane's thickness for membranes with minimum and maximum fiber diameter

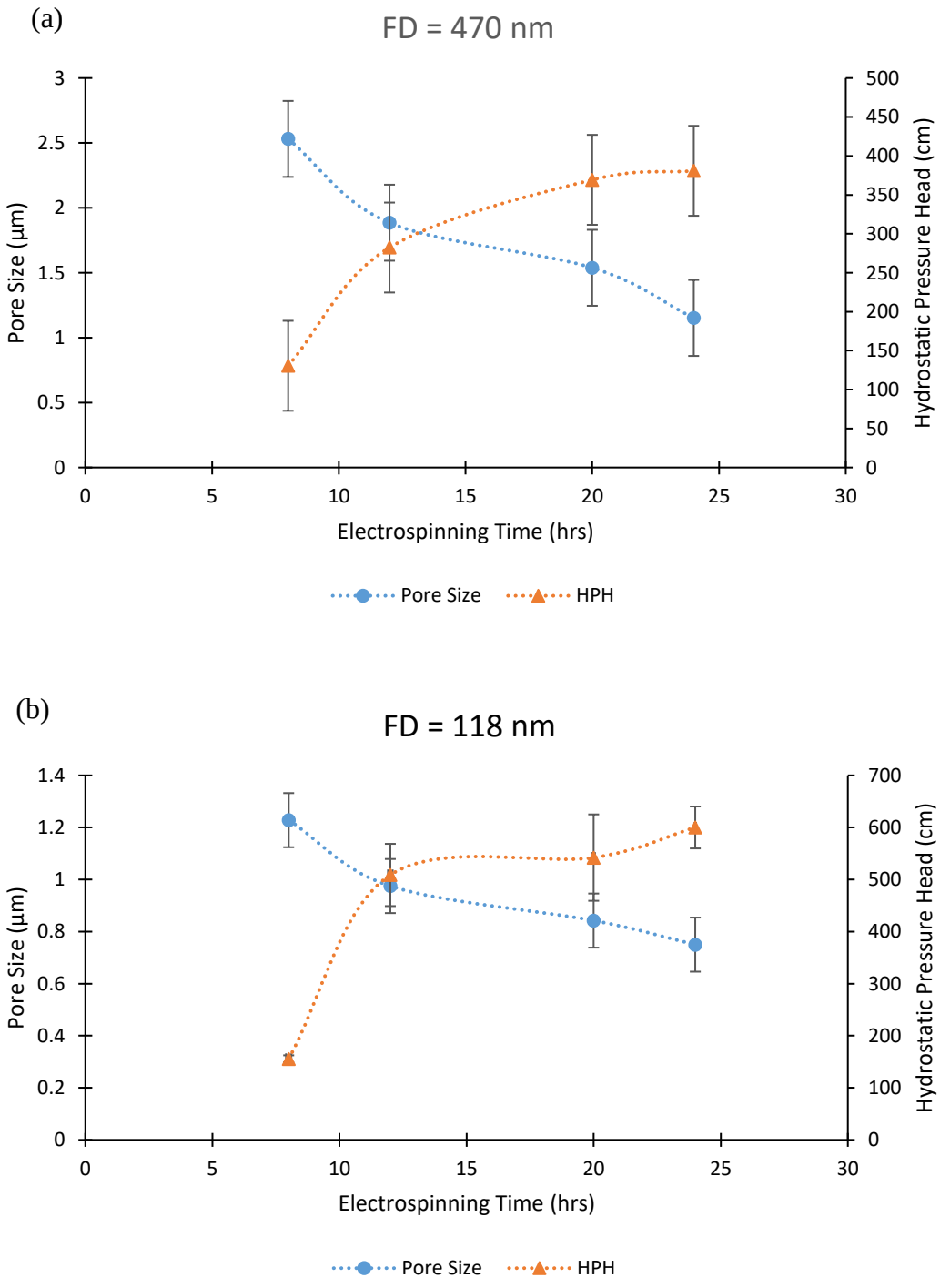

Figure 12. Effect of time of electrospinning on Pore size and HPH of the membrane with (a) maximum fiber diameter (FD = 470 nm), (b) minimum fiber diameter (FD = 118 nm)

Table 5. Properties of the Electrospun Membranes

Membrane	FD (nm)	Electrospinning Time (hr)	Pore size (μm)	HHP (cm)	Thickness (mm)
FD470t8	470	8	2.5 ± 0.01	130 ± 48.6	0.11 ± 0.02
FD470t12	470	12	1.8 ± 0.08	282 ± 25.5	0.15 ± 0.03
FD470t20	470	20	1.5 ± 0.02	369 ± 22.4	0.24 ± 0.01
FD118t8	118	8	1.2 ± 0.1	450 ± 12.9	0.17 ± 0.004
FD118t12	118	12	0.9 ± 0.09	508 ± 59.8	0.22 ± 0.015
FD118t20	118	20	0.8 ± 0.05	542 ± 82.9	0.33 ± 0.02

Thus, it is concluded that to obtain a membrane with the highest fiber diameter and pore size, the membrane should be electrospun with the following parameters: PVC wt% = 16, Voltage = 11 kV, TCD = 17 cm, F = 1 ml/h, DMF:THF = 62.5:37.5, and ES time = 8 hrs. In order to obtain a membrane with smallest fiber diameter and pore size, the membrane should be electrospun with the following parameters: PVC wt% = 12, Voltage = 17 kV, TCD = 11 cm, F = 1 ml/h, DMF:THF = 62.5:37.5, and ES time = 20 hrs. The SEM images shown in Figure 13 represent the interconnected bead-free nanofibrous structures of the membranes of minimum and maximum fiber diameter. It can be noticed that the fibers morphology of the membrane of FD=118 nm (Figure 13-a) constitutes a distribution of thin fibers that are highly interconnected and stacked forming small interfiber pores. In contrary, the fibers morphology

of the membrane of FD=480 nm (Figure 13-b) constitutes of thick fibers with large interfibers pores.

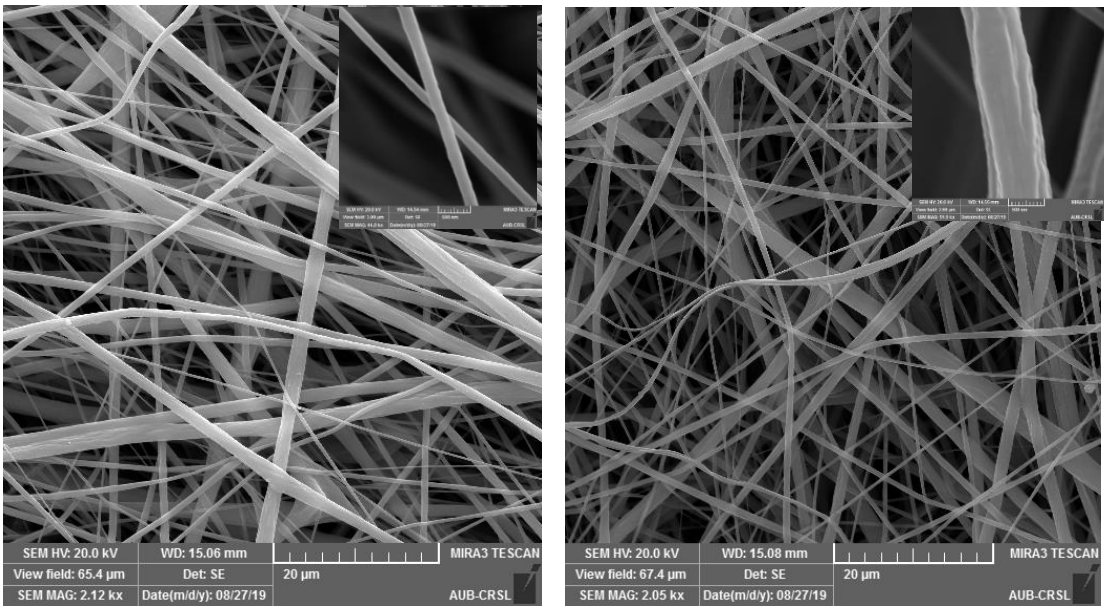

Figure 13 SEM Images of the Electrospun Membranes of Fiber Diameter (a) 118 nm and (b) 480 nm

B. Wettability Characteristics of the Original PVC Membrane

After controlling the fabrication parameters to obtain the desired membrane morphology, the wetting characteristics of the PVC membrane were tested under various conditions. The water contact angle of the membrane was $155^{o} \pm 2.7$ (Figure 14) while oil was wetting the membrane (OCA~0^{o}). This reflects the superhydrophobic and oleophilic nature of the PVC electrospun membrane. The superhydrophobicity of the membrane is attributed to the surface energy of the membrane, the chemical composition, and the hierarchical roughness of the surface. Moreover, the influence of the solution pH on the wettability of the membrane was evaluated. The contact angles of aqueous solutions with

different pH (1-11) were measured. Figure 15 shows that the WCA on the membrane were nearly unchanged at various pH, reflecting the strong durability of the surface against pH changes by acids and alkaline addition. Note that the water droplets were tinted in blue dye for the purpose of reflecting the different pH solutions. In addition, the resistance of the surface to salt solutions was analyzed. The contact angles of solutions with various salt concentrations (10-40 wt%) were measured. Figure 16 shows that the contact angles (similarly, the water droplets are tinted in red dye) also remained almost constant regardless of the NaCl concentration, demonstrating that the membrane's wettability can withstand the harsh solution conditions of seawater.

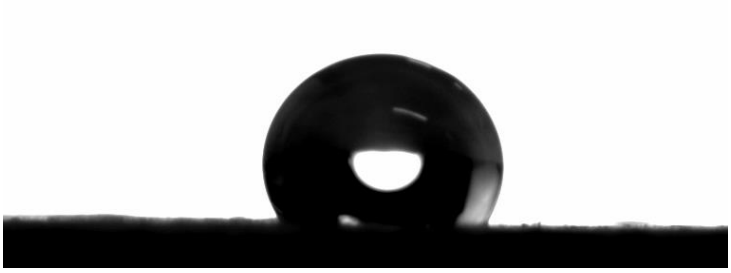

Figure 14. Water Contact Angle on Hydrophobic Membrane

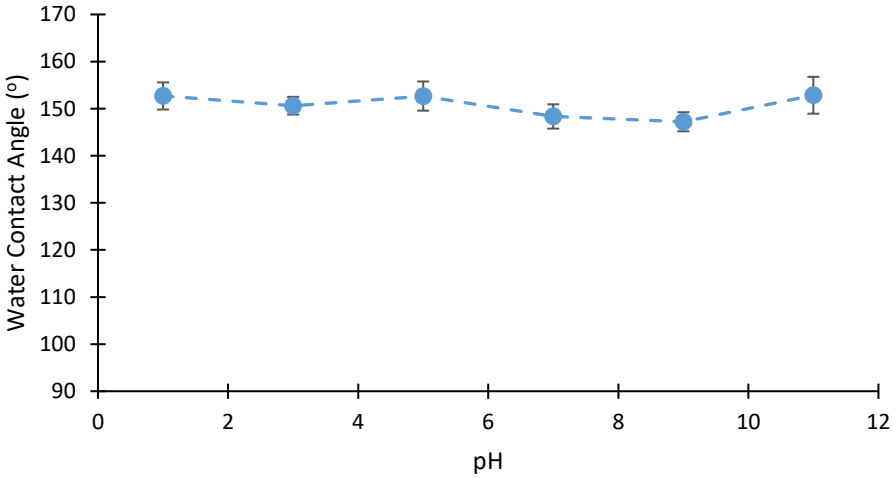

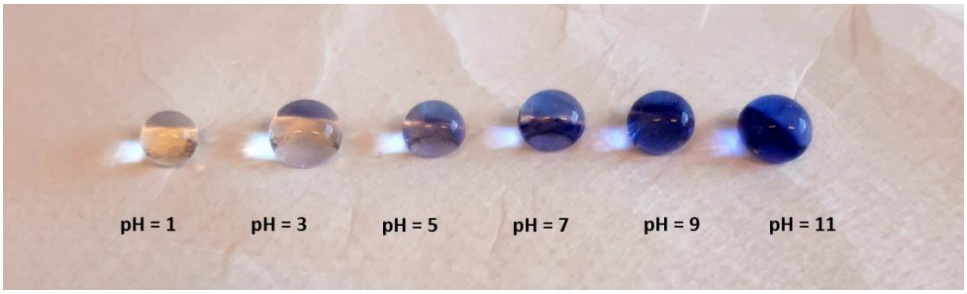

Figure 15 Effect of pH on membrane's water contact angle

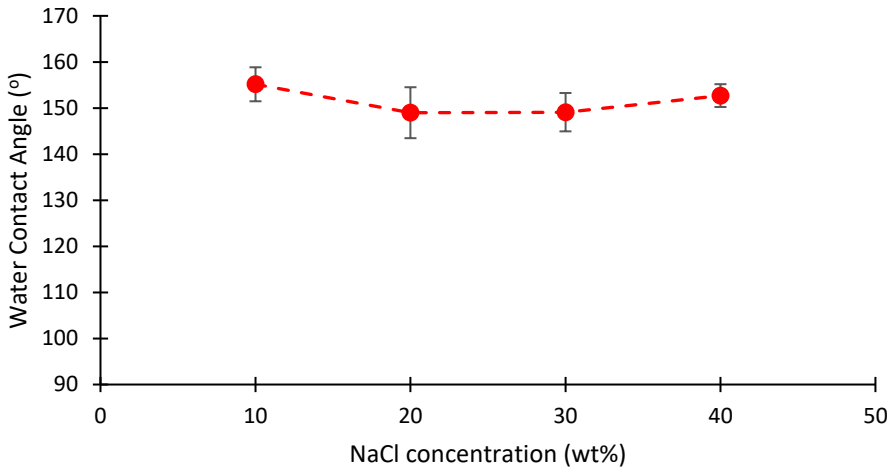

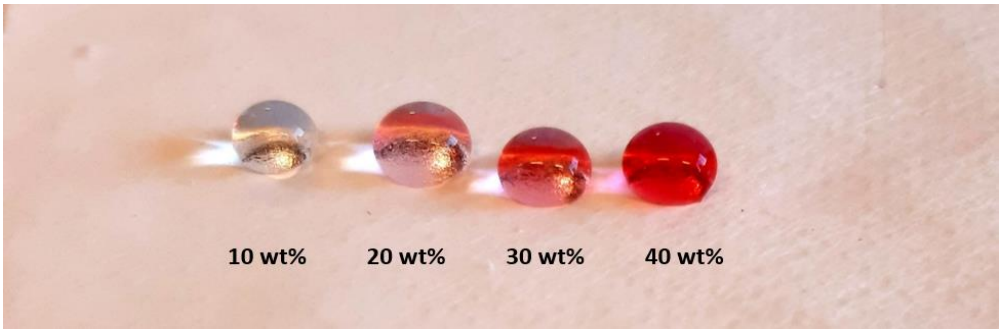

Figure 16. WCA on the electrospun membrane at various NaCL Concentrations

C. Surface Modification of the PVC Membrane

The major challenge of the present work was to develop a PVC membrane with versatile functionalities using simple and effective techniques. To achieve this, two novel approaches were adopted to surface modify the membranes altering their wettability to become hydrophilic/underwater oleophobic. To our knowledge, no one has cationized the PVC membrane surface using the cationizing agent Quat-188. Moreover, the

functionalization of PEI on the PVC chain has not been investigated for oil-water separation applications. The reaction schemes and mechanisms are presented in this section.

1. Modification Mechanisms

a. The reaction between PVC and Quat-188

The PVC membrane was first aminated using triethylenetetramine (TETA). The aminated PVC was then cationized using 3-chloro-2-hydroxypropyl trimethyl ammonium chloride (Quat-188). In the first reaction, triethylenetetramine (TETA) was used as a nucleophile to aminate PVC polymeric chain through an S_{N2} reaction. The carbon-containing chlorine is attacked by the N-atom displacing the chloride anion which then bonds with the left-over hydrogen forming the by-product hydrochloric acid. The resulting compound is the aminated PVC as shown below (Figure 17). In the second reaction, 3-chloro-2-hydroxypropyl trimethyl ammonium chloride (Quat-188) was used as the quaternary ammonium reagent. The cationization reaction involves multiple reaction steps occurring simultaneously in the presence of an alkali. NaOH solution was added in multiple steps during the reaction to catalyze the reaction and to neutralize the generated acid to accelerate the reaction. Upon the reaction of Quat-188 with NaOH, the chlorohydrin form of Quat-188 reagent is converted to an epoxide. The epoxy intermediate reacts with the amino groups of aminated PVC to introduce the quaternary ammonium substituent.

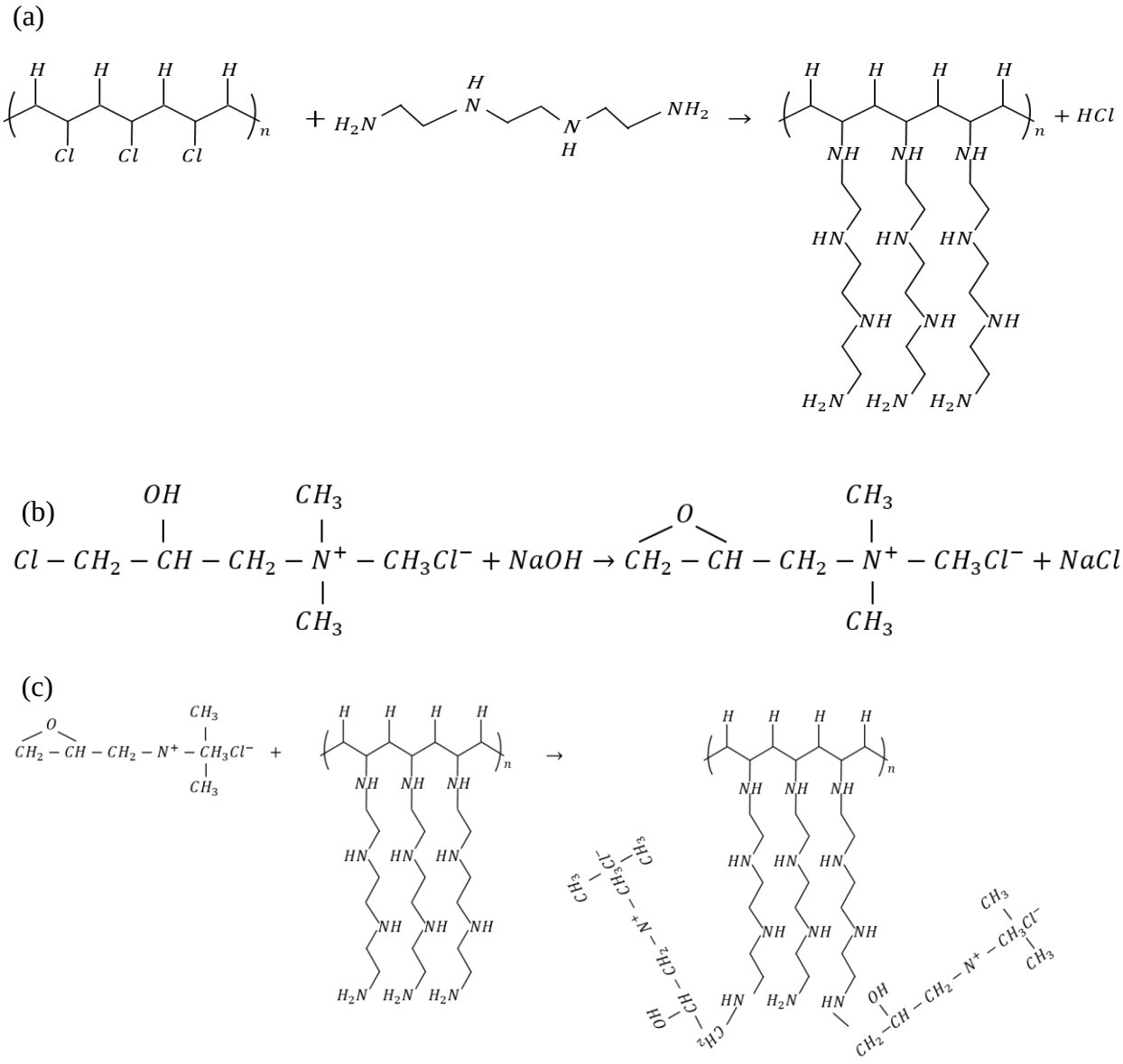

Figure 17 The reaction schemes of (a) Reaction 1: Reaction between PVC and TETA, (b) Reaction 2: Reaction between Quat-188 and NaOH, and (c) Reaction 3: Reaction between PVC and Quat-188.

b. <u>The reaction between PVC and PEI</u>

The reaction between PVC and PEI is a single step process as shown in Figure 18. An alkylation reaction occurs between the amine groups on PEI and the chlorines in PVC. PEI contains primary, secondary, and tertiary amines. However, due to the bulkiness of the branched polymer, reactions with the secondary and tertiary amines are less likely to occur due to the steric hindrance. Thus, the suggested reaction is the attack of the primary amine groups to the halogen chloride forming a cross-linked polymer.

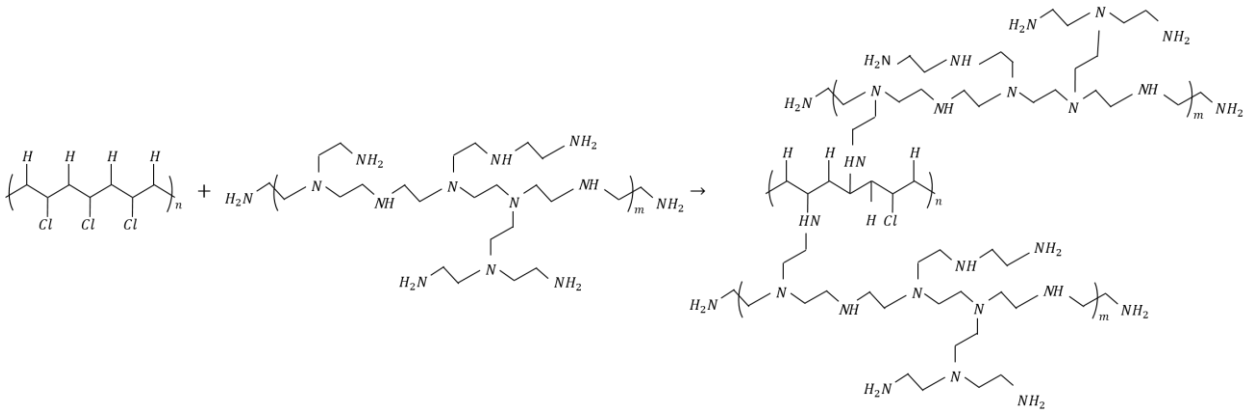

Figure 18. Reaction Scheme of PVC and PEI

D. Characterization of Modified Membranes

The morphology of the modified membranes can be seen in the SEM images (Figure 19). The fiber from the original PVC membrane appears to be rough and thin. The PEI- and Quat 188- modified membranes fibers appear to have micro- and nanoscale protrusions. This has increased the diameter of the membrane and its roughness.

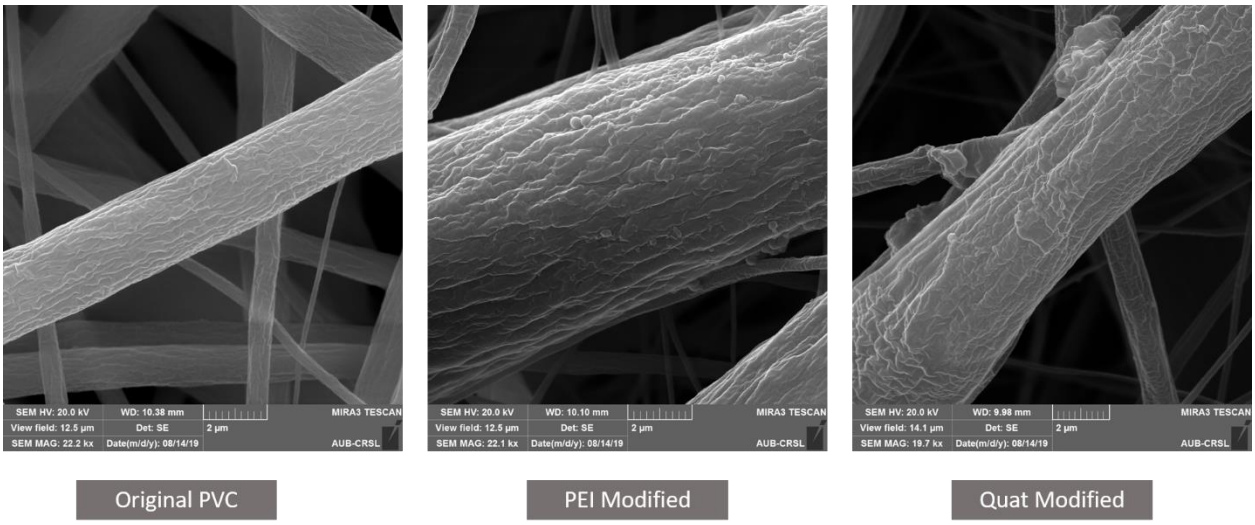

Figure 19. SEM images of the (a) Original PVC Membrane, (b) PEI-Modified Membrane, and (c) Quat-188-Modified Membrane

Moreover, a thermal gravimetric analysis was conducted for the original, Quat 188-modified, and PEI-modified PVC membranes as shown in

Figure 20. For the PVC membrane, the graph presented two-stage degradation pattern. The first weight loss was between 250 °C and 350 °C, which is attributed to the dehydrochlorination of PVC molecular chain. The second thermal degradation was between 430 °C and 500 °C, ascribing to the further degradation of the polyene chain (C-C bond) and the formation of aliphatic and aromatic compounds [46, 66]. In regards to the Quat 188-modified membrane, the TG curve presented an initial weight loss at 50 ^{o}C, which may be due to the low thermal stability of the quaternary groups grafted onto the PVC chain [66]. As for the PEI-modified membrane, the TG curve showed similar trends as that of the PVC membrane with a shift in the first thermogram to a lower temperature (50 °C) lower, which is due to the substitution of the chlorine with amino functional group [88].

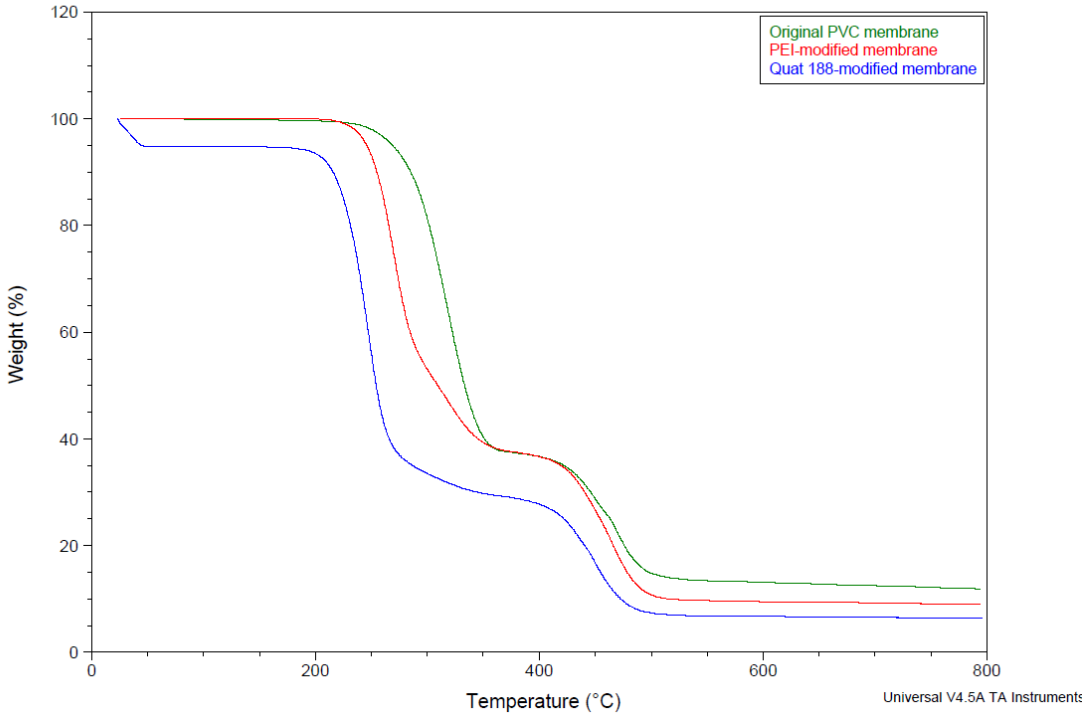

Figure 20. Thermal Gravimetric Analysis of the membranes

E. Wettability Characteristics of the Surface Modified Superhydrophilic/Underwater Superoleophobic Membrane

The wetting characteristics of the surface-modified membrane were characterized. When the contact angle was measured in the oil-water-membrane three-phase system, the membrane showed underwater superoleophobic property with OCA of $150^{o} \pm 2.3$ for the PEI-modified membrane and $152^{o} \pm 1.8$ for the Quat 188-modified membrane as shown in Figure 21. When the membrane was immersed in water, the amine and quaternary ammonium salts adsorb the water. The presence of bound water on the surface of the membrane led to the increase in the OCA underwater, rendering the membrane underwater superoleophobic.

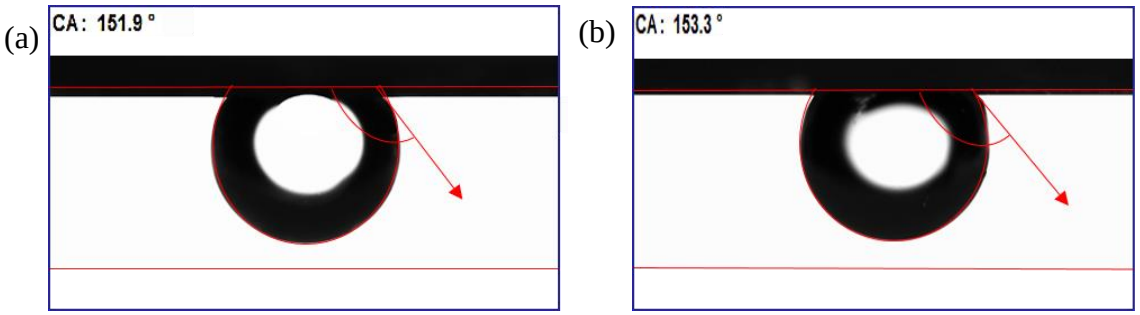

Figure 21 Underwater Oil Contact Angle for (a) PEI-modified membrane and (b) Quat-188-modified membrane

The modified membranes exhibited underwater superoleophobicity towards several oils (engine oil, vegetable oil, cyclohexane, toluene, and decane) as shown in Figure 22. The oil contact angle was greater than 135^{o} for the selected oil types and hydrocarbons. Moreover, the membrane had very low oil-adhesion. The oil droplet was suspended from the syringe and contacted with the surface. Afterwards, the syringe was lifted up. The oil droplet remained attached to the syringe and could hardly fall on the surface until it was placed on it by force. This reflects the low oil adhesion to the surface. Moreover, when the surface was tilted, the oil droplet rolls easily on the surface without any losses. The superoleophobicity of the membrane along with the low oil adhesion reflect the great potential of the membrane for oil-water separation.

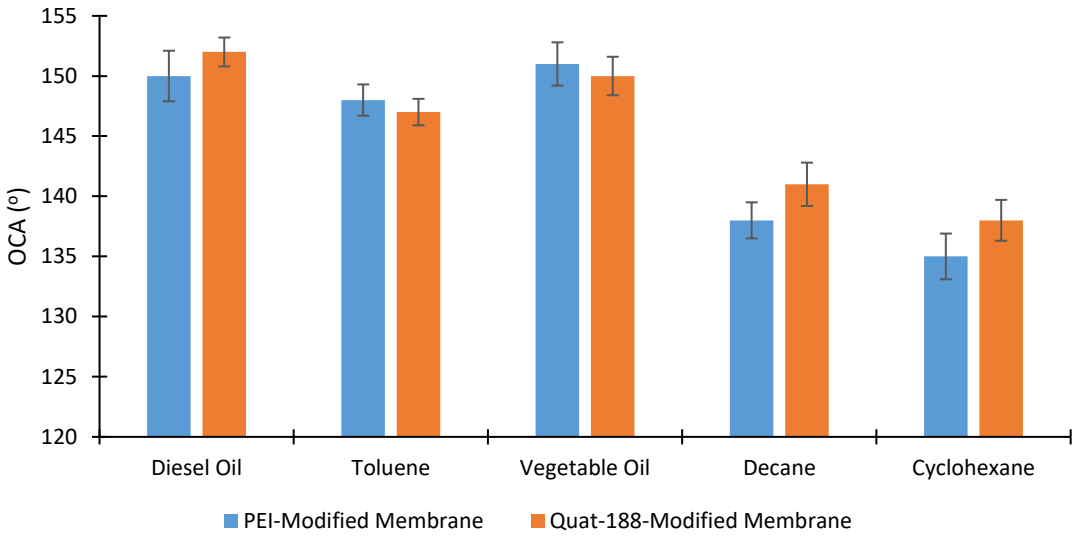

Figure 22 OCA of PEI- and Quat-188 Modified Membranes (FD470t20) for various oil types

To further understand the correlation between the hydrophilicity of the membrane and the underwater superoleophobicity, the relationships between the contact angle and surface properties were analyzed. Young's equation describes the contact angle of a liquid droplet on a solid surface in air. If the equation is extended to a liquid droplet on a solid surface in another liquid, the three-phase system equation is described by a modified Young's equation (Equation 3-b). Knowing that the interfacial tension of water-air is around 72 mN/m and that of diesel oil-air is around 27 mN/m, a hydrophilic surface leads to oleophobicity underwater.

The Cassie-Baxter model explains the effect of roughness on the contact angle. According to the model, the water trapped in the pores repels the oil droplet leading to the superoleophobic property. Thus, both the hydrophilicity of the membrane and the roughness of the surface are crucial factors for underwater superoleophobicity.

F. Oil-Water Separation Experiments

1. Superhydrophobic/Superoleophilic Membrane

c. Pressure-driven Experiments

The oil-water separation capacity of the membrane in relation to the membrane properties (fiber diameter and porosity) was tested. The produced membranes were divided into membranes of maximum fiber diameter (470 nm) of porosity ranges (2.5 – 1.8 μm) and minimum fiber diameter (118 nm) of porosity ranges (1.2 – 0.8 μm). The membranes were placed in the membrane holder, a mixture of diesel oil and water (100ml:100ml) was allowed to pass through, and the diesel oil outlet flow rate was measured. Figure 23 shows the volume of oil recovered (l/m^2) and separation efficiency (%) for the membranes. All membranes had a separation efficiency above 80% obtained after 45 minutes of the experiment, with the maximum value being 95% corresponding to the membrane with the largest porosity and fiber diameter (2.5 μm and 470 nm respectively). This suggests that PVC electrospun membrane is an efficient oil-water separation technique.

(a)

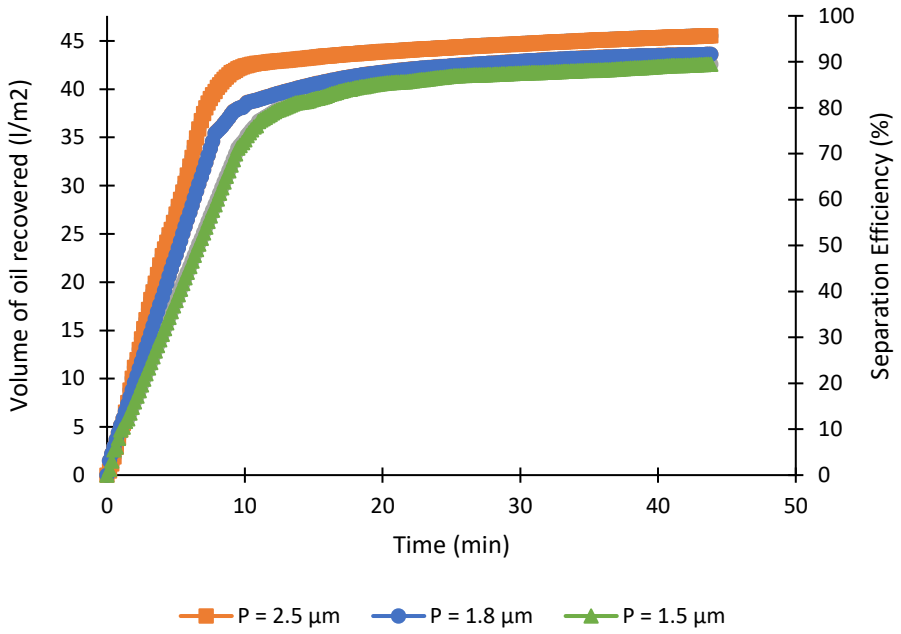

(b)

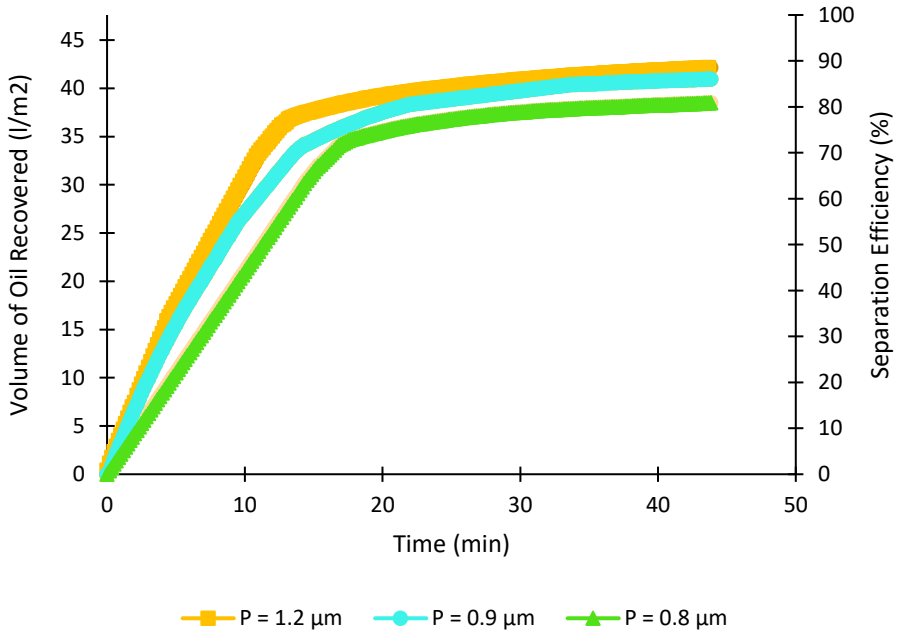

Figure 23 Volume of oil recovered (l/m2) vs time (min) for different pore sizes for (a) membrane with FD = 470 nm and (b) membrane with FD = 118 nm using diesel oil

All the membranes follow the same trend in oil-water separation. Initially, the oil recovery is very fast such that a minimum of 75% recovery is achieved within the first 10 minutes. As the oil is filtered and the water is recycled back to the main reservoir, the oil:water (v/v) ratio decreases, leading to the decrease in the separation slope. The initial slope of oil recovery along with the separation efficiency of the membranes within 10 and 40 minutes are reported in Table 6.

The results show that the oil-water separation flow rate increases with the increase of pore size and fiber diameter. This can be understood by analyzing the permeate flux of the porous membrane, described by Darcy's law (Equation 13)[89]:

$$J = \frac{3600\rho K}{\mu\delta}\Delta P \text{ (Eq. 13)}$$

Where J is the membrane flux (kg/ m^2 h), ρ is the density of the permeate (kg/m^3), K is the permeability, μ is the viscosity of the permeate (Pa s), δ is the membrane thickness (m), ΔP is the transmembrane pressure difference (Pa), and 3600 is to convert seconds to hour. Thus, the flux is directly related to the membrane's permeability, described by Carman-Kozney equation [89]:

$$K = \frac{d_f^2 \varepsilon^3}{16 k_{CK}(1-\varepsilon)^2} \text{ (Eq. 14)}$$

Where ε is the membrane porosity, d_f is the fiber diameter (m), and k_{CK} is the Carman-Kozney constant that is dependent on the structure of the membrane material. The membrane permeability is directly proportional to the square of the fiber diameter which explains the increase in the permeate flux with the fiber diameter.

Table 6 Initial Slope and Oil recovered after 10 mins and 40 mins

Membrane	**Initial Slope ($l/m^2.h$)**	**After 10 min**		**After 40 min**	
		Recovered Oil (l/m^2)	Separation Efficiency (%)	Recovered Oil (l/m^2)	Separation Efficiency (%)
FD470t8	584	42	89	45	95
FD470t12	523	38	81	43	91
FD470t20	419	35	73	42	89
FD118t8	344	30	64	42	88
FD118t12	298	27	57	41	86
FD118t20	253	21	44	38	80

d. Oil-only Gravity-driven Experiments

In order to study the oil permeation rate through the membrane, oils of various viscosities (diesel oil, decane, and cyclohexane) were allowed to pass through the membrane under the effect of gravity alone. Table 7 shows the properties of the used oils, whereby the viscosities were measured using the . Figure 24 shows the volume of oil recovered (ml/m^2) for diesel, cyclohexane, and decane.

Table 7 Oil Properties

Oil Name	**Viscosity (cP)**	**Density (g/ml)**
Diesel	18.2	0.8
Cyclohexane	0.98	0.779
Decane	0.859	0.73

(a)

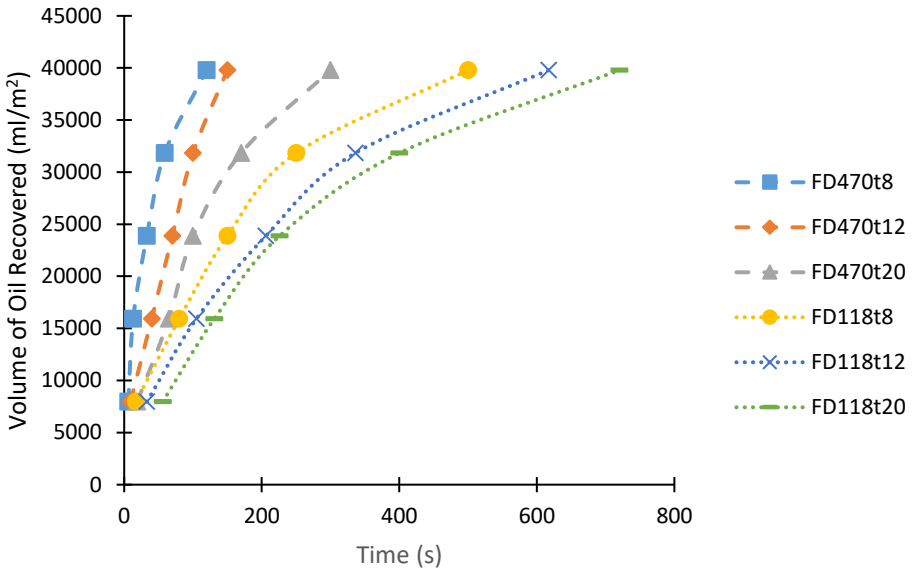
45000
40000
35000
30000
25000
20000
15000
10000
5000
0
Volume of Oil Recovered (ml/m²)
0
200
400
600
800
Time (s)
FD470t8
FD470t12
FD470t20
FD118t8
FD118t12
FD118t20

(b)

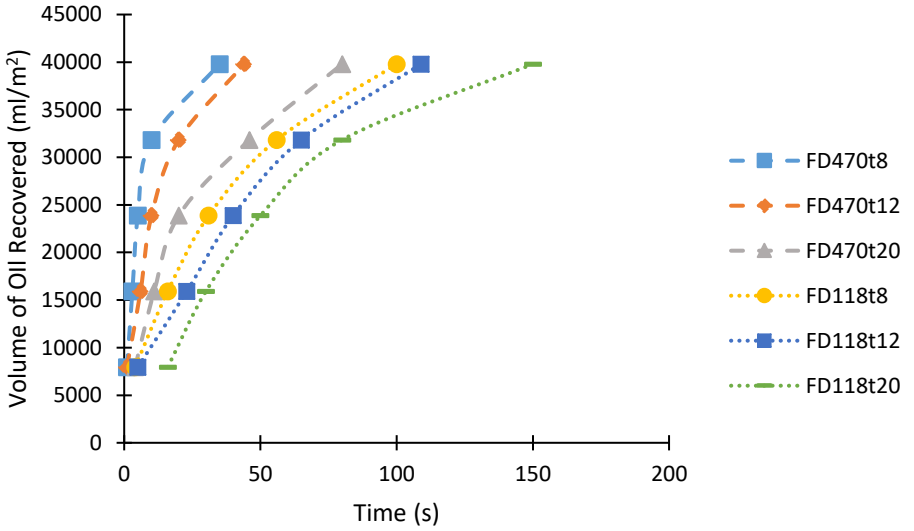
45000
40000
35000
30000
25000
20000
15000
10000
5000
0
Volume of OIl Recovered (ml/m²)
0
50
100
150
200
Time (s)
FD470t8
FD470t12
FD470t20
FD118t8
FD118t12
FD118t20

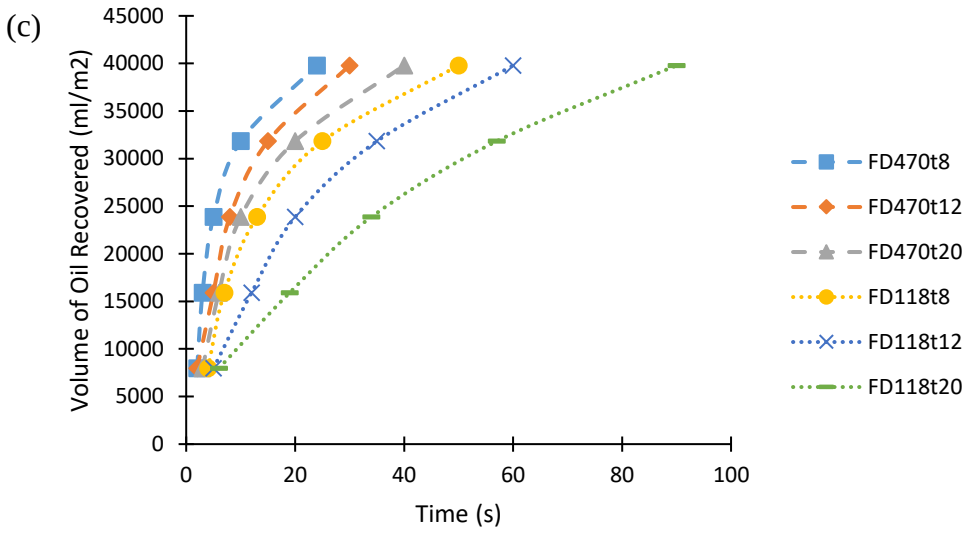

Figure 24 The volume of oil recovered (ml/m2) with time (s) for membranes of two fiber diameters (FD = 470 nm and 118 nm) using (a) diesel , (b) cyclohexane, and (c) decane.

The oil fluxes (l/m^2/h) are summarized in Table 8. The results show that the oil flux increases with the decrease in viscosity of the oil. For example, for the membrane of FD = 470 nm and pore size = 1.2 µm, the oil fluxes are 286.4, 1432.4, and 2469.6 for diesel oil, cyclohexane, and decane, respectively. This can be explained as well by Darcy's law (Equation 13) where the viscosity is inversely proportional to the permeate flux [89].

Table 8. Oil Flux for the membranes using diesel, cyclohexane, and decane

	Pore Size (µm)	**Oil Flux (l/m^2/h)**		
		Diesel	**Cyclohexane**	**Decane**
FD = 470 nm	**2.5**	1193.6	4092.5	5968.3
	1.8	954.9	3255.4	4774.6
	1.5	477.4	1507.7	2604.3
	1.2	286.4	1432.3	2469.6

FD = 118 nm	**0.9**	232.1	1314.1	2387.3
	0.8	198.9	954.9	1591.5

e. Membrane Durability

To assess the durability of the membrane, the separation experiment was repeated five times, each for 45 minutes. The separation efficiency remained the same after the five cycles (Figure 25). This proves the membrane's ability to be reused efficiently.

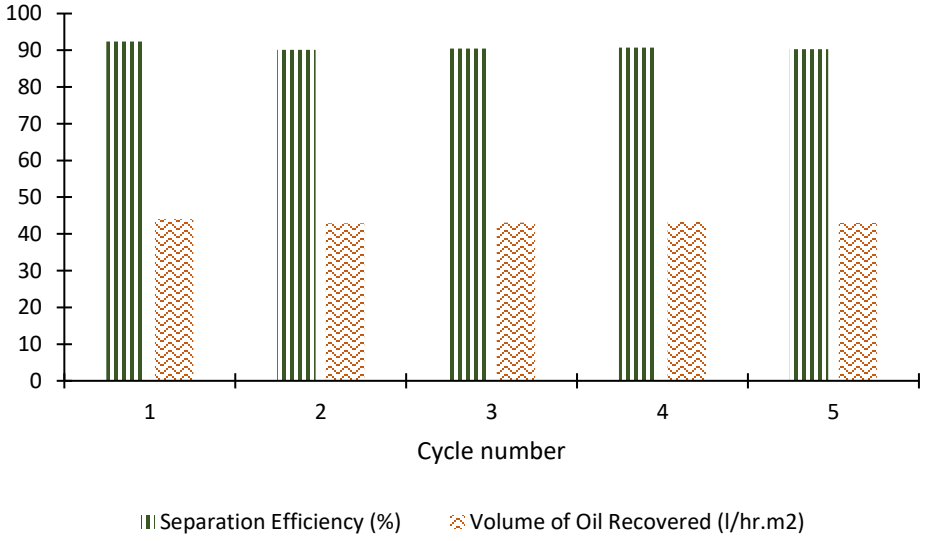

Figure 25 Durability of Membrane M12 during pressure-driven filtration using diesel oil

3. Superhydrophilic/Underwater Superoleophobic PVC Membrane

To evaluate the oil-water separation capacity of the surface-modified membranes, several oil-water separation experiments were conducted. Upon filtering a mixture of oil-water (50:50) with a total volume of 100 ml under gravity, water rapidly passed through the membrane and was collected in the beaker. Due to hydrophilic nature of the modified PVC membrane, the oil remained on top of the membrane and could not pass through the membrane as shown in Figure 26. The water separation flux and the efficiency separation for the modified PVC membranes were shown in Figure 28Figure 29. The separation efficiency reached a value above 99.9% for all types of oil for both membranes. However, the flux of the recovered water for the PEI-modified membranes was in the range of 1500-3000 l/(m^2h), while that of the Quat 188-modified membranes were in the range of 250-350 l/(m^2h). This may be attributed to two reasons. First, the Quat 188 modified membrane has undergone two heat treatments during the reaction processes which leads to the reduction in the pore sizes of the membranes. Second, once the water penetrates the Quat 188- modified surface, and due to its hygroscopic nature, a charged induced dipole bond is formed between the quaternary cationized salt and the water. The intermolecular potential energy needed to break this bond is much higher than that of a dipole-dipole bond that is formed upon the interaction between water and the amino functional group of the PEI. Accordingly, the time needed for the water to penetrate the Quat 188- modified membrane is longer and thus the flux is smaller.

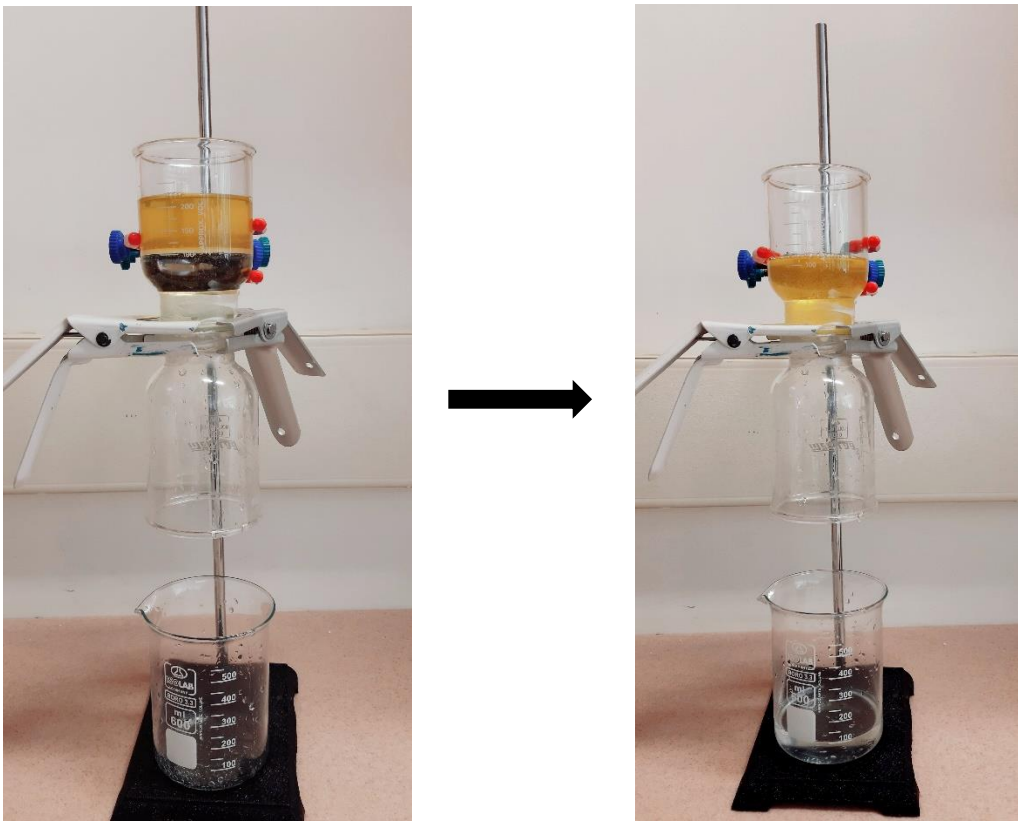

Figure 26 Diesel Oil-Water Separation using Superhydrophilic/Underwater SuperOleophobic (a) before, (b) after

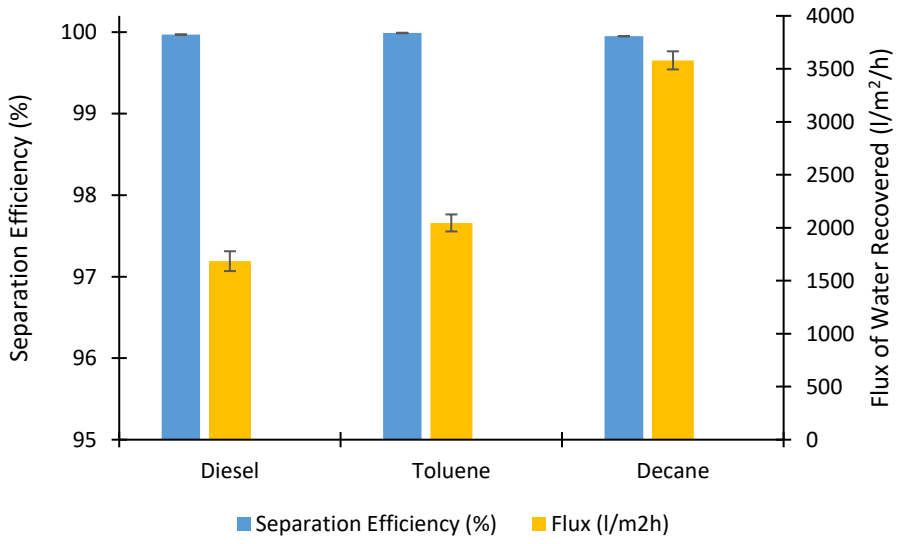

Figure 27 Separation Efficiency and Flux of Water Recovered for PEI- Surface Modified Membrane upon using various oil types

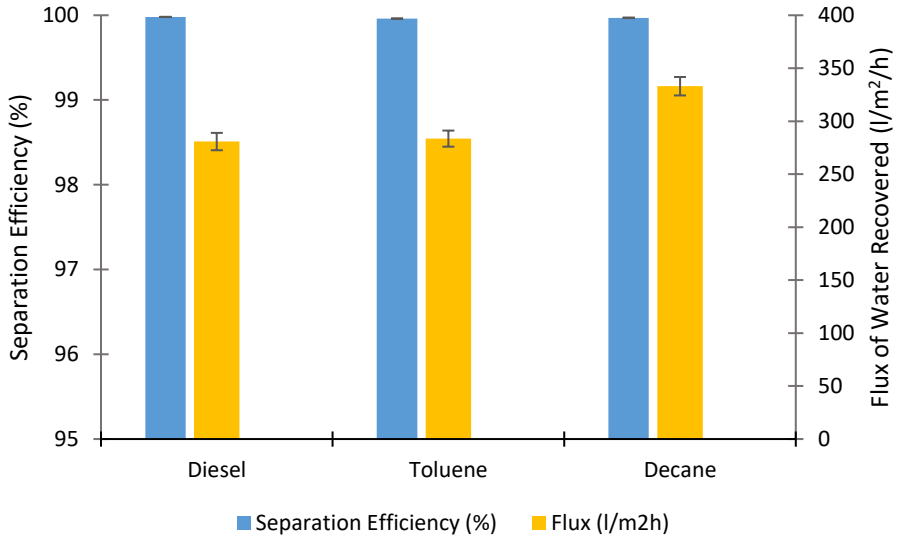

Figure 28 Separation Efficiency and Flux of Water Recovered for Quat-188 Surface Modified Membrane upon using various oil types

The reusability of the membranes was studied by repeating the separation experiment 10 times. The separation efficiency remained the same and no oil residuals were detected in the filtrate as shown in Figure 29.

The mentioned experiments prove that the surface-modified membranes possess the required characteristics for highly efficient oily wastewater treatment.

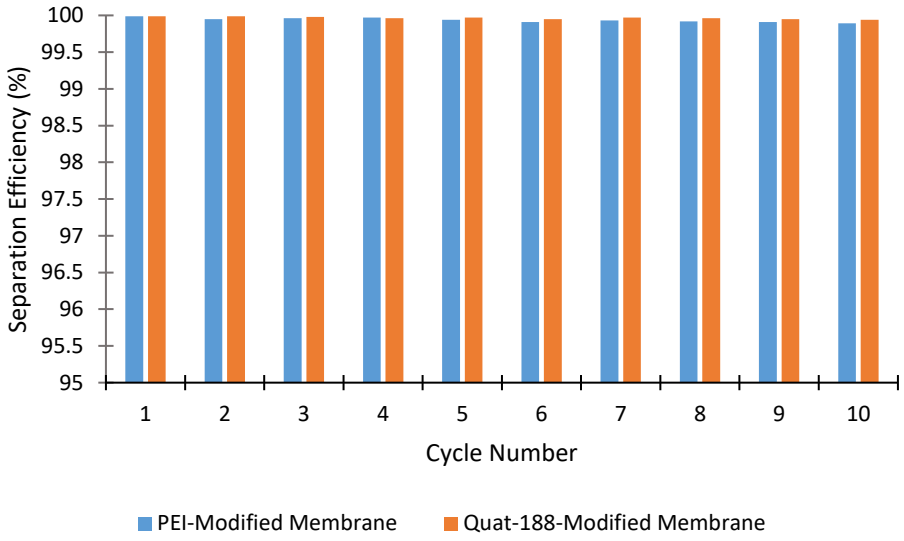

Figure 29 Separation Efficiency of the PEI- and Quat 188- Modified Membranes after 10 Cycles

CHAPTER V

CONCLUSION AND RECOMMENDATIONS

We have illustrated an efficient and robust method to fabricate a PVC membrane with dual functionality: “oil-removing” and “water-removing”. The optimization of the electrospinning parameters using response surface methodology contributed to the controlled production of membranes with optimum structural parameters for high separation efficiency. Upon electrospinning the membrane under the following conditions: [polymer] = 16 wt%, the solvent ratio DMF:THF = 62.5:37.5, polymer feed rate = 1 ml/h, voltage = 11 kV, tip to collector distance = 14 cm, drum speed = 500 rpm, and electrospinning time = 8 hr, membrane with maximum fiber diameter (470 nm) and pore size (2.5 µm) was obtained. The oil recovery was enhanced from 80% to 95% as the fiber diameter and pore size increase from 118 nm to 470 nm and 0.8 µm to 2.5 µm, respectively. The membrane maintained its wettability under acidic, alkali, and saline conditions. It proved to be durable and sustained its performance after 5 separation cycles, each run for 45 minutes. Moreover, we have demonstrated two novel, simple, and effective surface modification techniques. Both approaches, quaternizing the membrane surface or grafting it with amino groups, contributed to the simultaneous improvement of the membrane’s hydrophilicity and underwater oleophobicity. The separation efficiency for both membranes was above 99.9% upon using various oil and hydrocarbon types (diesel, toluene, cyclohexane, and decane). This performance persisted even after 10 separation cycles.

In conclusion, the presented work offers several advancements in membrane technology. The fabricated membrane proved to have high efficiency, chemical stability, and

durability. It is recommended for future work to investigate the mechanical stability of the membrane. Moreover, the surface modification of the membrane offered a robust method to overcome one of the key obstacles in membrane technology, fouling. To further demonstrate the robustness of the membrane, it is suggested to test its efficiency using real industrial waste. For future work, the designed membranes with antagonistic wettability properties, can be used simultaneously. The hydrophobic membrane allows the passage of oil and the hydrophilic membrane allows the passage of water. Thus, both the water and oil phases are treated, and the build-up of pressure due to the accumulation of either the water or oil is prevented. Upon the usage of this simple system, large volumes of oily wastewater with a wide variety of concentrations, may be separated efficiently.

CHAPTER VI

REFERENCES

[1] "Oil Tanker Spill Statistics 2018," ITOPF2019.

[2] R. K. Gupta, G. J. Dunderdale, M. W. England, and A. Hozumi, "Oil/water separation techniques: a review of recent progresses and future directions," *Journal of Materials Chemistry A,* vol. 5, no. 31, pp. 16025-16058, 2017.

[3] S. Putatunda, S. Bhattacharya, D. Sen, and C. Bhattacharjee, "A review on the application of different treatment processes for emulsified oily wastewater," *International Journal of Environmental Science and Technology,* vol. 16, no. 5, pp. 2525-2536, 2018.

[4] A. Fakhru'l-Razi, A. Pendashteh, L. C. Abdullah, D. R. Biak, S. S. Madaeni, and Z. Z. Abidin, "Review of technologies for oil and gas produced water treatment," *J Hazard Mater,* vol. 170, no. 2-3, pp. 530-51, Oct 30 2009.

[5] M. Padaki *et al.*, "Membrane technology enhancement in oil–water separation. A review," *Desalination,* vol. 357, pp. 197-207, 2015.

[6] C. An, G. Huang, Y. Yao, and S. Zhao, "Emerging usage of electrocoagulation technology for oil removal from wastewater: A review," *Sci Total Environ,* vol. 579, pp. 537-556, Feb 1 2017.

[7] H. J. Tanudjaja, C. A. Hejase, V. V. Tarabara, A. G. Fane, and J. W. Chew, "Membrane-based separation for oily wastewater: A practical perspective," *Water Res,* vol. 156, pp. 347-365, Jun 1 2019.

[8] J. M. Dickhout, J. Moreno, P. M. Biesheuvel, L. Boels, R. G. H. Lammertink, and W. M. de Vos, "Produced water treatment by membranes: A review from a colloidal perspective," *Journal of Colloid and Interface Science,* vol. 487, pp. 523-534, 2017/02/01/ 2017.

[9] Z. Zhong, Q. Cao, B. Jing, X. Wang, X. Li, and H. Deng, "Electrospun PVdF–PVC nanofibrous polymer electrolytes for polymer lithium-ion batteries," *Materials Science and Engineering: B,* vol. 177, no. 1, pp. 86-91, 2012/01/25/ 2012.

[10] F. E. Ahmed, B. S. Lalia, and R. Hashaikeh, "A review on electrospinning for membrane fabrication: Challenges and applications," *Desalination,* vol. 356, pp. 15-30, 2015.

[11] P. Bosiger *et al.*, "Application of response surface methodology to tailor the surface chemistry of electrospun chitosan-poly(ethylene oxide) fibers," *Carbohydr Polym,* vol. 186, pp. 122-131, Apr 15 2018.

[12] Q. You, G. Ran, C. Wang, Y. Zhao, and Q. Song, "Facile fabrication of superhydrophilic and underwater superoleophobic chitosan–polyvinyl alcohol-TiO2 coated copper mesh for efficient oil/water separation," *Journal of Coatings Technology and Research,* vol. 15, no. 5, pp. 1013-1023, 2018.

[13] W. Ma *et al.*, "Electrospun fibers for oil–water separation," *RSC Advances,* vol. 6, no. 16, pp. 12868-12884, 2016.

[14] S. Jafarinejad, "Treatment of Oily Wastewater," pp. 185-267, 2017.

[15] K. KRÄMER. (2018). *Oil Spill Cleanup*. Available: https://www.chemistryworld.com/features/oil-spill-cleanup/3008990.article
[16] S. Jamaly, A. Giwa, and S. W. Hasan, "Recent improvements in oily wastewater treatment: Progress, challenges, and future opportunities," *J Environ Sci (China)*, vol. 37, pp. 15-30, Nov 1 2015.
[17] B. Song and Q. Xu, "Highly Hydrophobic and Superoleophilic Nanofibrous Mats with Controllable Pore Sizes for Efficient Oil/Water Separation," *Langmuir*, vol. 32, no. 39, pp. 9960-9966, 2016.
[18] Y. Zhu, D. Wang, L. Jiang, and J. Jin, "Recent progress in developing advanced membranes for emulsified oil/water separation," *Npg Asia Materials*, Review vol. 6, p. e101, 05/23/online 2014.
[19] B. S. Lalia, V. Kochkodan, R. Hashaikeh, and N. Hilal, "A review on membrane fabrication: Structure, properties and performance relationship," *Desalination*, vol. 326, pp. 77-95, 2013/10/01/ 2013.
[20] X. Wang, J. Yu, G. Sun, and B. Ding, "Electrospun nanofibrous materials: a versatile medium for effective oil/water separation," *Materials Today*, vol. 19, no. 7, pp. 403-414, 2016.
[21] M. Montazer and T. Harifi, "9 - Nanofinishes for self-cleaning textiles," in *Nanofinishing of Textile Materials*, M. Montazer and T. Harifi, Eds.: Woodhead Publishing, 2018, pp. 127-143.
[22] Y. Q. Liu, Y. L. Zhang, X. Y. Fu, and H. B. Sun, "Bioinspired Underwater Superoleophobic Membrane Based on a Graphene Oxide Coated Wire Mesh for Efficient Oil/Water Separation," *ACS Appl Mater Interfaces*, vol. 7, no. 37, pp. 20930-6, Sep 23 2015.
[23] S. K. Hong, S. Bae, H. Jeon, M. Kim, S. J. Cho, and G. Lim, "An underwater superoleophobic nanofibrous cellulosic membrane for oil/water separation with high separation flux and high chemical stability," *Nanoscale*, vol. 10, no. 6, pp. 3037-3045, Feb 8 2018.
[24] J. Yong *et al.*, "Bioinspired underwater superoleophobic surface with ultralow oil-adhesion achieved by femtosecond laser microfabrication," *Journal of Materials Chemistry A*, 10.1039/C4TA01277A vol. 2, no. 23, pp. 8790-8795, 2014.
[25] X. Gao *et al.*, "Dual-scaled porous nitrocellulose membranes with underwater superoleophobicity for highly efficient oil/water separation," *Adv Mater*, vol. 26, no. 11, pp. 1771-5, Mar 19 2014.
[26] W. Zhang *et al.*, "Salt-Induced Fabrication of Superhydrophilic and Underwater Superoleophobic PAA-g-PVDF Membranes for Effective Separation of Oil-in-Water Emulsions," *Angewandte Chemie International Edition*, vol. 53, no. 3, pp. 856-860, 2014.
[27] D. Wu *et al.*, "Facile creation of hierarchical PDMS microstructures with extreme underwater superoleophobicity for anti-oil application in microfluidic channels," *Lab on a Chip*, 10.1039/C1LC20226J vol. 11, no. 22, pp. 3873-3879, 2011.
[28] M. A. Gondal, M. S. Sadullah, M. A. Dastageer, G. H. McKinley, D. Panchanathan, and K. K. Varanasi, "Study of Factors Governing Oil–Water Separation Process Using TiO2 Films Prepared by Spray Deposition of Nanoparticle Dispersions," *ACS Applied Materials & Interfaces*, vol. 6, no. 16, pp. 13422-13429, 2014/08/27 2014.

[29] N. Wang, A. Raza, Y. Si, J. Yu, G. Sun, and B. Ding, "Tortuously structured polyvinyl chloride/polyurethane fibrous membranes for high-efficiency fine particulate filtration," *Journal of Colloid and Interface Science*, vol. 398, pp. 240-246, 2013/05/15/ 2013.

[30] *Poly(vinyl chloride)*. Available: https://www.sigmaaldrich.com/catalog/product/aldrich/389323?lang=en&region=LB

[31] F. P. Reding, E. R. Walter, and F. J. Welch, "Glass transition and melting point of poly(vinyl chloride)," *Journal of Polymer Science*, vol. 56, no. 163, pp. 225-231, 1962.

[32] (2003). *Coefficients of Linear Thermal Expansion*. Available: https://www.engineeringtoolbox.com/linear-expansion-coefficients-d_95.html

[33] T. Ahmad, C. Guria, and A. Mandal, "Optimal synthesis and operation of low-cost polyvinyl chloride/bentonite ultrafiltration membranes for the purification of oilfield produced water," *Journal of Membrane Science*, vol. 564, pp. 859-877, 2018.

[34] Y. Su, Q. Zhao, J. Liu, J. Zhao, Y. Li, and Z. Jiang, "Improved oil/water emulsion separation performance of PVC/CPVC blend ultrafiltration membranes by fluorination treatment," *Desalination and Water Treatment*, vol. 55, no. 2, pp. 304-314, 2014.

[35] W. S. Khan, N. U. Khan, and M. M. Janjua, *Wastewater Treatment with PVC Electrospun Nanofibrous Membrane*. 2019, pp. 1-6.

[36] X. Wang and B. S. Hsiao, "Electrospun nanofiber membranes," *Current Opinion in Chemical Engineering*, vol. 12, pp. 62-81, 2016.

[37] S. Mohammadzadehmoghadam, Y. Dong, and I. J. Davies, "Modeling electrospun nanofibers: An overview from theoretical, empirical, and numerical approaches," *International Journal of Polymeric Materials and Polymeric Biomaterials*, vol. 65, no. 17, pp. 901-915, 2016.

[38] B. E.-s. a. E.-s. Services. *Electrospinning Process Bionicia*. Available: https://bioinicia.com/electrospinning-equipment-fiber-fabrication/electrospinning-process-bioinicia/

[39] K. H. Lee, H. Y. Kim, Y. M. La, D. R. Lee, and N. H. Sung, "Influence of a mixing solvent with tetrahydrofuran andN,N-dimethylformamide on electrospun poly(vinyl chloride) nonwoven mats," *Journal of Polymer Science Part B: Polymer Physics*, vol. 40, no. 19, pp. 2259-2268, 2002.

[40] X. Zhu, X. Jiang, S. Cheng, K. Wang, S. Mao, and L.-J. Fan, "Preparation of high strength ultrafine polyvinyl chloride fibrous membrane and its adsorption of cationic dye," *Journal of Polymer Research*, vol. 17, no. 6, pp. 769-777, 2009.

[41] C. Carrizales *et al.*, "Thermal and mechanical properties of electrospun PMMA, PVC, Nylon 6, and Nylon 6,6," *Polymers for Advanced Technologies*, vol. 19, no. 2, pp. 124-130, 2008.

[42] A. Zulfi, Y. A. Rezeki, D. Edikresnha, M. M. Munir, and K. Khairurrijal, "Synthesis of Fibers and Particles from Polyvinyl Chloride (PVC) Waste Using Electrospinning," *IOP Conference Series: Materials Science and Engineering*, vol. 367, p. 012014, 2018.

[43] B. Tarus, N. Fadel, A. Al-Oufy, and M. El-Messiry, "Effect of polymer concentration on the morphology and mechanical characteristics of electrospun cellulose acetate and poly (vinyl chloride) nanofiber mats," *Alexandria Engineering Journal*, vol. 55, no. 3, pp. 2975-2984, 2016.
[44] N. Xu, J. Cao, and Y. Lu, "Electrospun polyvinyl chloride/poly (butyl methacrylate-co-butyl acrylate) fibrous mat for absorption of organic matters," *Iranian Polymer Journal*, vol. 25, no. 3, pp. 251-262, 2016.
[45] H. Zhu, S. Qiu, W. Jiang, D. Wu, and C. Zhang, "Evaluation of electrospun polyvinyl chloride/polystyrene fibers as sorbent materials for oil spill cleanup," *Environ Sci Technol*, vol. 45, no. 10, pp. 4527-31, May 15 2011.
[46] M. H. Othman, M. Mohamed, and I. Abdullah, "Electrospinning of PVC with natural rubber," pp. 926-931, 2013.
[47] R. Asmatulu, M. Ceylan, and N. Nuraje, "Study of superhydrophobic electrospun nanocomposite fibers for energy systems," *Langmuir*, vol. 27, no. 2, pp. 504-7, Jan 18 2011.
[48] H. Hong, Z. C. Tronstad, Y. Yang, and M. D. Green, "Characterization of PVC-soy protein nonwoven mats prepared by electrospinning," *AIChE Journal*, vol. 64, no. 7, pp. 2737-2744, 2018.
[49] Z. Zhong, Q. Cao, X. Wang, N. Wu, and Y. Wang, "PVC–PMMA composite electrospun membranes as polymer electrolytes for polymer lithium-ion batteries," *Ionics*, vol. 18, no. 1-2, pp. 47-53, 2011.
[50] Z. Zhong, Q. Cao, B. Jing, S. Li, and X. Wang, "Novel electrospun PAN–PVC composite fibrous membranes as polymer electrolytes for polymer lithium-ion batteries," *Ionics*, vol. 18, no. 9, pp. 853-859, 2012.
[51] M. Ahmadipourroudposht, E. Fallahiarezoudar, N. M. Yusof, and A. Idris, "Application of response surface methodology in optimization of electrospinning process to fabricate (ferrofluid/polyvinyl alcohol) magnetic nanofibers," *Mater Sci Eng C Mater Biol Appl*, vol. 50, pp. 234-41, May 2015.
[52] D. Baş and İ. H. Boyacı, "Modeling and optimization I: Usability of response surface methodology," *Journal of Food Engineering*, vol. 78, no. 3, pp. 836-845, 2007.
[53] R. H. Myers, D. C. Montgomery, and C. M. Anderson-Cook, *Response Surface Methodology : Process and Product Optimization Using Designed Experiments* (no. Book, Whole). New York: John Wiley & Sons, Incorporated, 2016.
[54] M. Support. *What are response surface designs, central composite designs, and Box-Behnken designs?* Available: https://support.minitab.com/en-us/minitab/18/help-and-how-to/modeling-statistics/doe/supporting-topics/response-surface-designs/response-surface-central-composite-and-box-behnken-designs/
[55] Y. Peng and Y. Sui, "Compatibility research on PVC/PVB blended membranes," *Desalination*, vol. 196, no. 1, pp. 13-21, 2006/09/05/ 2006.
[56] J. Xu and Z.-L. Xu, "Poly(vinyl chloride) (PVC) hollow fiber ultrafiltration membranes prepared from PVC/additives/solvent," *Journal of Membrane Science*, vol. 208, no. 1, pp. 203-212, 2002/10/01/ 2002.
[57] M. H. Davood Abadi Farahani, H. Rabiee, V. Vatanpour, and S. M. Borghei, "Fouling reduction of emulsion polyvinylchloride ultrafiltration membranes blended by PEG:

the effect of additive concentration and coagulation bath temperature," *Desalination and Water Treatment,* vol. 57, no. 26, pp. 11931-11944, 2016.

[58] T. Ahmad, C. Guria, and A. Mandal, "Synthesis, characterization and performance studies of mixed-matrix poly(vinyl chloride)-bentonite ultrafiltration membrane for the treatment of saline oily wastewater," *Process Safety and Environmental Protection,* vol. 116, pp. 703-717, 2018/05/01/ 2018.

[59] Y. Zhang, X. Tong, B. Zhang, C. Zhang, H. Zhang, and Y. Chen, "Enhanced permeation and antifouling performance of polyvinyl chloride (PVC) blend Pluronic F127 ultrafiltration membrane by using salt coagulation bath (SCB)," *Journal of Membrane Science,* vol. 548, pp. 32-41, 2018/02/15/ 2018.

[60] E. Demirel, B. Zhang, M. Papakyriakou, S. Xia, and Y. Chen, "Fe2O3 nanocomposite PVC membrane with enhanced properties and separation performance," *Journal of Membrane Science,* vol. 529, pp. 170-184, 2017/05/01/ 2017.

[61] A. Behboudi, Y. Jafarzadeh, and R. Yegani, "Preparation and characterization of TiO2 embedded PVC ultrafiltration membranes," *Chemical Engineering Research and Design,* vol. 114, pp. 96-107, 2016/10/01/ 2016.

[62] H. Rabiee, V. Vatanpour, M. H. D. A. Farahani, and H. Zarrabi, "Improvement in flux and antifouling properties of PVC ultrafiltration membranes by incorporation of zinc oxide (ZnO) nanoparticles," *Separation and Purification Technology,* vol. 156, pp. 299-310, 2015/12/17/ 2015.

[63] A. Farouk, S. Sharaf, and M. M. Abd El-Hady, "Preparation of multifunctional cationized cotton fabric based on TiO2 nanomaterials," *Int J Biol Macromol,* vol. 61, pp. 230-7, Oct 2013.

[64] A. Wang, Q. Zhu, and Z. Xing, "A functionalized chitosan wrinkled hollow sphere containing calcium ions: Efficient adsorption of sodium dodecylbenzenesulfonate (SDBS) from aqueous solutions," *J Colloid Interface Sci,* vol. 555, pp. 203-213, Jul 29 2019.

[65] M. Palencia, T. A. Lerma, and N. Afanasjeva, "Antibacterial cationic poly(vinyl chloride) as an approach for in situ pathogen-inactivation by surface contact with biomedical materials," *European Polymer Journal,* vol. 115, pp. 212-220, 2019/06/01/ 2019.

[66] C. Wu, Z. Wang, S. Liu, Z. Xie, H. Chen, and X. Lu, "Simultaneous permeability, selectivity and antibacterial property improvement of PVC ultrafiltration membranes via in-situ quaternization," *Journal of Membrane Science,* vol. 548, pp. 50-58, 2018/02/15/ 2018.

[67] J. A. Brydson, "26 - Epoxide Resins," in *Plastics Materials (Seventh Edition)*, J. A. Brydson, Ed. Oxford: Butterworth-Heinemann, 1999, pp. 744-777.

[68] V. Vatanpour and N. Haghighat, "Improvement of polyvinyl chloride nanofiltration membranes by incorporation of multiwalled carbon nanotubes modified with triethylenetetramine to use in treatment of dye wastewater," *Journal of Environmental Management,* vol. 242, pp. 90-97, 2019/07/15/ 2019.

[69] J. Zhu *et al.*, "Improved Antifouling Properties of Poly(vinyl chloride) Ultrafiltration Membranes via Surface Zwitterionicalization," *Industrial & Engineering Chemistry Research,* vol. 53, no. 36, pp. 14046-14055, 2014.

[70] Y. M. Feng, Z. L. Du, T. Zheng, and P. Wang, "Modification of jute by use of triethylenetetramine and its ad-sorption behavior for copper (II)," in *First International Conference on Information Sciences, Machinery, Materials and Energy*, 2015: Atlantis Press.

[71] Y. P. Han and Q. Lin, "Synthesis,Characterization, and Antibacterial Activity of Quaternized of N-Aromatic Chitosan Derivatives," *Applied Mechanics and Materials*, vol. 138-139, pp. 1202-1208, 2011.

[72] G. E. Evans, J. Shore, and C. V. Stead, "Dyeing Behaviour of Cotton after Pretreatment with Reactive Quaternary Compounds," *Journal of the Society of Dyers and Colourists*, vol. 100, no. 10, pp. 304-315, 1984.

[73] H. N. Park, H. A. Choi, and S. W. Won, "Fibrous polyethylenimine/polyvinyl chloride crosslinked adsorbent for the recovery of Pt(IV) from acidic solution: Adsorption, desorption and reuse performances," *Journal of Cleaner Production*, vol. 176, pp. 360-369, 2018.

[74] M. S. Sajab, C. H. Chia, S. Zakaria, and P. S. Khiew, "Cationic and anionic modifications of oil palm empty fruit bunch fibers for the removal of dyes from aqueous solutions," *Bioresource Technology*, vol. 128, pp. 571-577, 2013/01/01/ 2013.

[75] V. V. Goncharuk, L. N. Puzyrnaya, G. N. Pshinko, A. A. Bogolepov, and V. Ya. Demchenko, "The removal of heavy metals from aqueous solutions by montmorillonite modified with polyethylenimine," *Journal of Water Chemistry and Technology*, vol. 32, pp. 67-72, 04/01 2010.

[76] Y. Ma, W.-J. Liu, N. Zhang, Y.-S. Li, H. Jiang, and G.-P. Sheng, "Polyethylenimine modified biochar adsorbent for hexavalent chromium removal from the aqueous solution," *Bioresource technology*, vol. 169C, pp. 403-408, 07/10 2014.

[77] H. A. Choi, H. N. Park, and S. W. Won, "A reusable adsorbent polyethylenimine/polyvinyl chloride crosslinked fiber for Pd(II) recovery from acidic solutions," *J Environ Manage*, vol. 204, no. Pt 1, pp. 200-206, Dec 15 2017.

[78] Y. Avny and D. Porath, "Polyethylenimine—Poly(vinyl Chloride) Crosslinked Polymers and Their Use in Adsorption of Mercuric and Cupric Salts," *Journal of Macromolecular Science: Part A - Chemistry*, vol. 10, no. 6, pp. 1193-1203, 1976.

[79] R. Jurdi, L. Zaidouny, M. Abou-Daher, A. R. Tehrani-Bagha, N. Ghaddar, and K. Ghali, "Electrospun polymer blend with tunable structure for oil-water separation," *Journal of Applied Polymer Science*, vol. 135, no. 48, p. 46890, 2018.

[80] J. Wang, Y. Li, H. Tian, J. Sheng, J. Yu, and B. Ding, "Waterproof and breathable membranes of waterborne fluorinated polyurethane modified electrospun polyacrylonitrile fibers," *RSC Advances*, 10.1039/C4RA09129A vol. 4, no. 105, pp. 61068-61076, 2014.

[81] N. Bhardwaj and S. C. Kundu, "Electrospinning: a fascinating fiber fabrication technique," *Biotechnol Adv*, vol. 28, no. 3, pp. 325-47, May-Jun 2010.

[82] N. Amiri, A. Moradi, S. A. S. Tabasi, and J. Movaffagh, "Modeling and process optimization of electrospinning of chitosan-collagen nanofiber by response surface methodology," *Materials Research Express*, vol. 5, no. 4, 2018.

[83] P. Agarwal, P. K. Mishra, and P. Srivastava, "Statistical optimization of the electrospinning process for chitosan/polylactide nanofabrication using response

surface methodology," *Journal of Materials Science,* journal article vol. 47, no. 10, pp. 4262-4269, May 01 2012.

[84] H. Shao, J. Fang, H. Wang, and T. Lin, "Effect of electrospinning parameters and polymer concentrations on mechanical-to-electrical energy conversion of randomly-oriented electrospun poly(vinylidene fluoride) nanofiber mats," *RSC Advances,* 10.1039/C4RA16360E vol. 5, no. 19, pp. 14345-14350, 2015.

[85] D. I. M Yusuf Ansari, Dr S J A Rizvi, "Effects Of Processing Parameters On Morphology Of Polyvinyl Alcohol Based Electrospun Nano Fiber," *International Journal of Scientific & Engineering Research,* vol. 8, no. 7, 2017.

[86] A. Haider, S. Haider, and I.-K. Kang, "A comprehensive review summarizing the effect of electrospinning parameters and potential applications of nanofibers in biomedical and biotechnology," *Arabian Journal of Chemistry,* vol. 11, no. 8, pp. 1165-1188, 2018.

[87] W. Ding, S. Wei, J. Zhu, X. Chen, D. Rutman, and Z. Guo, "Manipulated Electrospun PVA Nanofibers with Inexpensive Salts," *Macromolecular Materials and Engineering,* vol. 295, no. 10, pp. 958-965, 2010.

[88] M. Mohy Eldin *et al.*, "Click Grafting of Chitosan onto PVC Surfaces for Biomedical Applications," *Advances in Polymer Technology,* vol. 37, 02/01 2018.

[89] M. M. Tomadakis and T. J. Robertson, "Viscous Permeability of Random Fiber Structures: Comparison of Electrical and Diffusional Estimates with Experimental and Analytical Results," *Journal of Composite Materials,* vol. 39, no. 2, pp. 163-188, 2005.